VisAidMath: Benchmarking Visual-Aided Mathematical Reasoning

Anonymous ACL submission

Abstract

Although previous research on large language models (LLMs) and large multi-modal models (LMMs) has systematically explored mathematical problem-solving (MPS) within visual contexts, the analysis of how these models process visual information during problem-solving remains insufficient. To address this gap, we present VisAidMath, a benchmark for evaluating the MPS process related to visual information. We follow a rigorous data curation pipeline involving both automated processes and manual annotations to ensure data quality and reliability. Consequently, this benchmark includes 1,200 challenging problems from various mathematical branches, vision-aid formulations, and difficulty levels, collected from diverse sources such as textbooks, examination papers, and Olympiad problems. Based on the proposed benchmark, we conduct comprehensive evaluations on ten mainstream LLMs and LMMs, highlighting deficiencies in the visual-aided reasoning process. For example, GPT-4V only achieves 45.33% accuracy in the direct visual-aided reasoning task, even with a drop of 2 points when provided with golden visual aids. In-depth analysis reveals that the main cause of deficiencies lies in hallucination regarding the implicit visual reasoning process, shedding light on future research directions in the visual-aided MPS process. We will host an evaluation platform at CodaBench[1] for testing publicly.

1 Introduction

Mathematical problem-solving (MPS) remains a significant hurdle for Large Language Models (LLMs) and Large Multi-modal Models (LMMs) (Hendrycks et al., 2021; Lewkowycz et al., 2022; Wu et al., 2020, 2021). The complexity intensifies when problems are presented in a multi-modal format, often involving visual elements alongside text (Lindström and Abraham, 2022; Masry et al., 2022). While some research has explored multi-modal MPS by incorporating visual contexts (Masry et al., 2022; Lu et al., 2023), these efforts predominantly focus on traditional vision-language task paradigms. Consequently, they tend to evaluate text-only reasoning steps, often underutilizing the visual information crucial for complex reasoning. This creates a significant gap between evaluating surface-level, text-only reasoning and true cross-modal reasoning, a gap our work aims to address as illustrated in Figure 1.

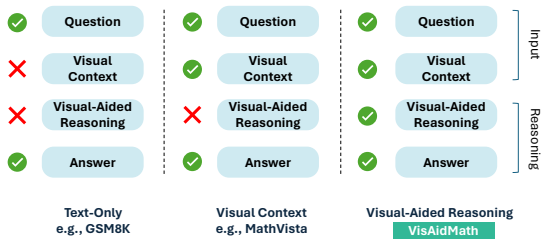

Figure 1: Comparison between VisAidMath and other benchmarks. Our work particularly focus on utilization of explicit and implicit visual context during reasoning process.

To bridge this gap, we introduce **VisAidMath**, a benchmark specifically designed to compel and evaluate the process of visual-aided mathematical reasoning. Drawing from diverse, high-quality sources, VisAidMath consists of 1,200 problems structured to necessitate the generation or utilization of visual aids, such as adding auxiliary lines in a geometry problem as an integral part of the solution process. This design moves beyond simple visual comprehension to directly target a model's ability to perform complex spatial and logical deductions grounded in visual context.

However, demonstrating the unique value of such a benchmark requires a more nuanced evaluation than what standard accuracy metrics can provide. Final answer correctness alone often masks underlying procedural flaws, failing to distinguish

[1] Our benchmark will be publicly released.

between genuine reasoning and fortunate shortcuts. To this end, we propose a **three-layered funnel evaluation framework** that moves beyond simple accuracy (ACCU) to assess **Process-Verified Accuracy (PVA)**, which filters out answers from flawed reasoning, and the **Solution Process Robustness Score (SPRS)**, which quantifies the fine-grained quality of a valid solution.

Applying this rigorous framework reveals a universal **"reasoning illusion"**: a dramatic collapse in performance from seemingly high accuracy to poor process quality across all tested models. Crucially, our experiments demonstrate that this illusion is most pronounced when models are confronted with the core tasks of VisAidMath. For instance, even the most advanced models, including GPT-4V and o1-mini, exhibit a staggering drop in performance when their reasoning steps are scrutinized, revealing fundamental weaknesses in generating and utilizing visual aids that standard metrics completely fail to capture. The visual aids generated by these SOTA models show minimal resemblance to human-provided solutions, highlighting a significant deficiency in their visual reasoning capabilities.

This paper's contributions are therefore threefold: (1) We introduce **VisAidMath**, a novel benchmark that mandates visual-aided reasoning for mathematical problem-solving. (2) We propose a new **evaluation framework** that uncovers the widespread "reasoning illusion" in current SOTA models. (3) Through comprehensive analysis, we provide quantitative proof that VisAidMath is uniquely effective at exposing these deep-seated reasoning failures, thereby establishing its value and pinpointing critical areas for the future development of more robust and reliable multi-modal models.

2 *VisAidMath*

2.1 Data Creation

Principles A typical problem within our *VisAidMath* benchmark comprises four parts: **Visual Context (C)**, **Question (Q)**, **Visual Aids (V)**, and **Answer (A)**. The main task involves prompting the model to generate visual aids that assist in mathematical reasoning. While the visual context may be optional, spatial descriptions are included as essential data elements within the question. Given that many text-based LLMs lack image understanding or generation capabilities, we have additionally annoatated precise captions for both the visual context and the visual aids through annotation. This allows us to extend the evaluation scenarios to models that are constructed with limited modality. By providing these detailed captions, we can accommodate models with varying modality capabilities.

Data Sources We collected the VisAidMath benchmark from both English and Chinese sources. Acknowledging the larger pool of mathematical problems with visual aids within the Chinese community, we primarily gathered data from these sources and subsequently applied machine translation. All data sources were categorized to ensure a balanced range of difficulty. A comprehensive description of our data sources, collection methodology, metadata, and translation process is detailed in B.2 and B.1.

Mathematical Categories To ensure diversity and balance, we manually collected and annotated a range of categories within the benchmark. Detailed categories and examples from different categorizations can be found in section C.

Construction Pipeline As depicted in Figure 6, We propose a construction pipeline for the VisAidMath dataset, which incorporates multi-round verification and dynamic quality control based on feedback. The dataset creation pipeline involves four key roles:

- `Administrator`: This role assigns daily collection tasks based on the progress and previous annotation feedback.
- `Collector`: The collector searches for data that satisfies the assigned collection tasks. The collected data should be in PDF format and later transformed into LaTeX files using OCR.
- `Annotator`: The annotator first validates and refines the LaTeX files by comparing the original PDF files provided by the collector with the transformed LaTeX files. Then, the annotator performs interactive labeling using our designed tool. To ensure a balanced distribution across different categories, the annotator regularly analyzes the data distribution and provides feedback on the current progress and any annotation issues to the collector and administrator.
- `Verifier`: The verifier is responsible for validating the categorization and data quality. If

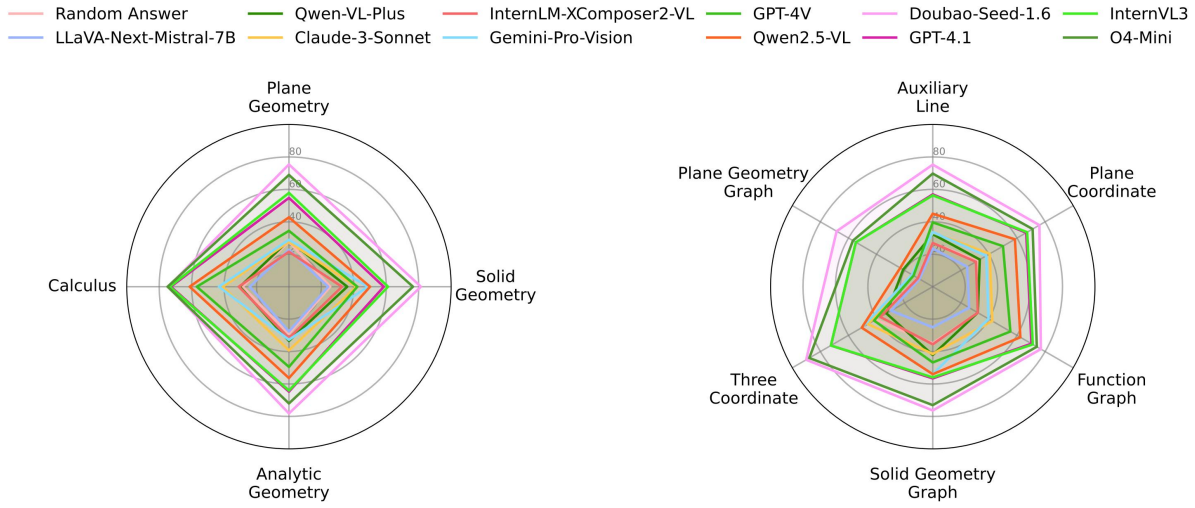

(a) Mathematical Branch

(b) Visual Aid

Figure 2: Accuracies of all LMM on visual-aided mathematical reasoning task across four branches and six visual aids. The best performing GPT-4V cannot exceed 60% accuracy score.

labels are not appropriate, they adjust the annotated captions of the context and visual aids.

To prepare the benchmark for wide English research community, we perform machine translation, data processing, and release preparation. The detailed processes can be found in Appendix D. Detail annotation process can be found at appendix D.1

2.2 Benchmark Attributes

The distribution of data sources is presented in Figure 8, providing a comprehensive overview of the dataset's origins. Additionally, the mathematical branches within the dataset exhibit a well-balanced distribution. This balance enables a broader exploration of diverse mathematical knowledge. It is worth noting that the distribution of visual aids labels is slightly imbalanced. This occurs because mathematics problems often involve overlapping types, and basic elements such as auxiliary lines are frequently incorporated as necessary components within more complex visual aids. Further details on the distribution of visual aid types can be found in Appendix C.2. Find other detail attributes in Appendix B.

2.3 Task Definition

Our work introduces a series of novel mathematical reasoning tasks centered on the use of visual aids. To formalize these tasks, we first define their basic components: the visual context (C), the textual question (Q), and the final answer (A). Crucially, a visual aid (V) in our framework is a **textual description** of a geometric construction, such as "Draw a line connecting point A and B." This allows us to evaluate a model's ability to reason about such aids without requiring image generation.

We establish a baseline task, **General Reasoning (GR)**, and introduce two novel formulations based on how visual aids are utilized: **Direct Visual-Aided Reasoning (D-VAR)**, which involves generating a visual aid, and **Indirect Visual-Aided Reasoning (I-VAR)**, which involves leveraging a provided one. The formal definitions and core distinctions of these three tasks are summarized in Table 1.

To accommodate language models that only accept textual inputs, the visual context 'C' is replaced by its textual description, denoted as C_{txt}. This creates text-only variants for each task, such as $(C_{\text{txt}}, Q) \rightarrow A$ for the GR task. This approach ensures a fair comparison across both multimodal and text-only models, as the visual aids themselves are consistently represented as text in all settings.

As defined in Table 1, the introduction of the D-VAR and I-VAR tasks distinguishes VisAidMath from traditional benchmarks. Unlike tasks that only require understanding existing visual elements, our approach compels models to engage in a deeper, two-step reasoning process: first by planning or in-

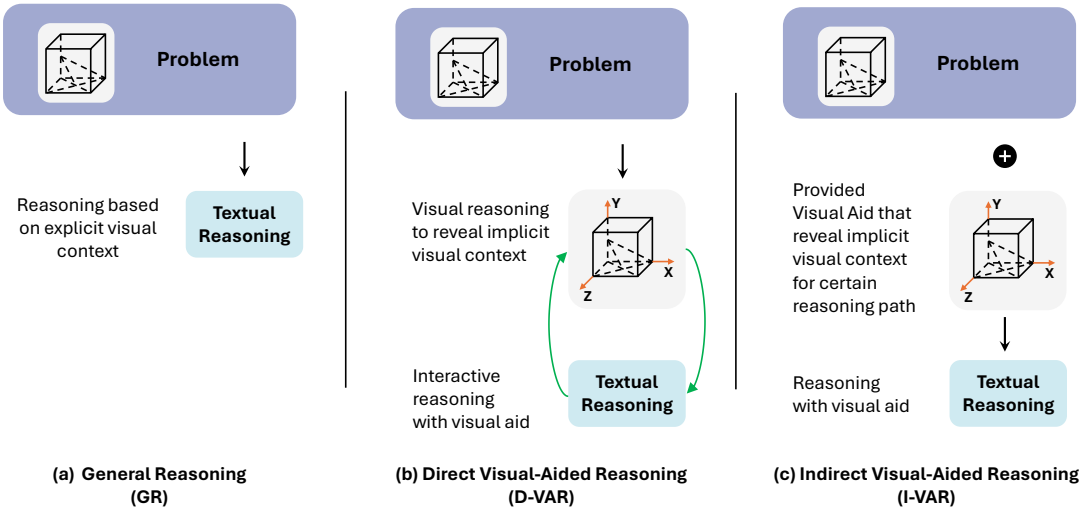

Figure 3: Comparison of different tasks: a) General Reasoning: provide MPS reasoning steps directly. b) Direct Visual-Aided Reasoning: create visual aids that disclose implicit visual context within problem, incorporating with textual reasoning to solve mathematical problem. c) Indirect Reasoning: solve the mathematical problem based on given visual aids. Direct visual-aided reasoning require the model to perform visual reasoning for visual aids generation.

Task Name	Abbr.	Formal Expression	Core Characteristic
General Reasoning	GR	$(C, Q) \rightarrow A$	Directly solves the problem.
Direct Visual-Aided Reasoning	D-VAR	$(C, Q) \rightarrow (V_g, A)$	**Generates** a visual aid to assist reasoning.
Indirect Visual-Aided Reasoning	I-VAR	$(C, Q, V_p) \rightarrow A$	**Utilizes** a provided visual aid for reasoning.

Table 1: Formal definitions of the reasoning tasks. V_g denotes a generated visual aid (output), while V_p denotes a provided visual aid (input).

terpreting geometric constructions (the visual aids), and then by executing the subsequent reasoning steps. This novel modality, focused on the generation and utilization of textual visual aids, allows us to specifically probe the spatial and logical planning capabilities of MLLMs. We illustrate the distinctions between these tasks in Figure 3.

3 Experiments

3.1 Models

To comprehensively evaluate the challenges posed by VisAidMath, we selected a wide spectrum of models, encompassing both leading open-source and proprietary systems. Our evaluation includes: 1) Open-source LLMs: Llama-2-7B (Touvron et al., 2023), Mistral-7B-Instruct-v0.2 (Jung et al., 2010); 2) Closed-source LLMs: GPT-3.5-turbo (OpenAI, 2023b), GPT-4-turbo (OpenAI, 2023c); 3) Open-source LMMs: LLaVA-Next-Mistral-7B (Liu et al., 2024a), InternLM-XComposer2-VL (Dong et al., 2024), VL-Cogito(), Qwen2.5-VL-72B(Bai et al., 2025), InternVL3.5-38B(Wang et al., 2025); 4) Closed-source LMMs: Qwen-VL-Plus (Bai et al., 2023), Gemini-Pro-Vision (Google, 2023), Claude-3-Sonnet (Anthropic, 2024), GPT-4-Vision (OpenAI, 2023a), GPT-4.1(OpenAI, 2023d), o4-mini(OpenAI, 2023e), and Doubao-seed-1.6(Guo et al., 2025). This extensive selection allows for a robust analysis of performance trends across different model architectures, scales, and training paradigms. Detailed experimental settings and hyperparameters are provided in Appendix E.1.

3.2 Three-Layered Funnel Evaluation

To move beyond surface-level correctness and enable a deeper assessment of mathematical reasoning, we introduce **The Three-Layered Funnel Evaluation Framework**. This hierarchical methodology is designed to scrutinize model outputs with increasing rigor at each successive layer. This approach allows us to distinguish not only correct from incorrect answers, but also robustly derived solutions from those that are superficially correct but procedurally flawed.

Final Answer Correctness (ACCU) Given that VisAidMath comprises mathematics problems with

Model	ALL	PLG	SDG	AYG	CAL	AXL	RTC	THC	PLG	SDG	FUG
Heuristics Baselines											
Random Answer	24.42	21.54	34.31	21.45	20.07	24.44	20.87	35.16	10.53	32.89	21.50
Frequent Answer	40.83	28.92	50.65	40.36	44.22	32.79	47.25	74.73	20.00	47.73	44.53
Large Language Models (LLMs): Text-Only Input											
Llama2-7B	26.83	21.85	34.64	30.55	20.75	26.68	25.23	39.56	11.58	30.26	26.49
Mistral-7b-Instruct-v0.2	27.42	27.38	30.72	27.64	23.81	27.57	28.21	28.57	11.58	27.63	26.87
GPT3.5	37.58	32.31	42.16	37.45	38.78	37.56	38.30	40.66	13.68	42.11	38.20
GPT4	51.92	41.54	52.29	50.91	63.95	45.75	54.59	60.44	23.16	53.29	61.23
Large Multimodal Models (LMMs): Text-Only Input											
LLaVA-Next-Mistral-7B	23.08	21.23	22.55	25.45	23.47	22.21	23.62	25.27	8.42	26.32	25.34
InternLM-XComposer2-VL	33.17	24.62	44.12	32.36	31.97	30.40	33.03	46.15	10.53	41.45	34.17
Qwen-VL-Plus	34.75	30.15	43.46	33.82	31.63	34.43	34.63	48.35	21.05	44.74	32.63
Gemini-Pro-Vision	38.42	31.08	48.37	31.27	42.86	34.72	37.84	49.45	18.95	51.97	39.54
Claude-3-Sonnet	38.58	31.38	43.46	39.27	40.82	36.66	40.14	46.15	14.74	43.42	42.23
GPT4V	47.00	35.08	47.06	50.55	56.80	41.43	50.69	48.35	15.79	47.37	55.66
Large Multimodal Models (LMMs): Multimodal Input											
LLaVA-Next-Mistral-7B	24.58	22.77	24.18	27.64	24.15	23.55	24.54	29.67	9.47	25.00	25.91
InternLM-XComposer2-VL	29.00	21.54	32.68	31.64	30.95	26.97	30.73	37.36	10.53	35.53	32.05
Qwen-VL-Plus	32.00	28.62	35.95	33.45	30.27	32.34	33.49	32.97	21.05	42.11	32.05
Gemini-Pro-Vision	38.33	28.92	48.69	32.73	43.20	33.68	38.07	50.55	14.74	53.95	39.73
Claude-3-Sonnet	37.08	27.69	41.50	39.27	40.82	33.38	40.60	46.15	14.74	41.45	42.42
GPT4V	45.33	34.46	42.16	49.45	56.80	39.64	50.00	41.76	13.68	46.71	55.28
VL-Cogito	49.17	40.31	53.92	53.74	49.45	45.31	53.85	52.40	55.26	50.23	20.00
Qwen2.5-VL-72B	52.25	42.77	50.00	61.22	56.36	45.01	50.55	62.38	53.95	58.49	23.16
GPT4.1	62.42	54.77	58.50	72.79	64.73	56.93	72.53	70.25	56.58	66.51	54.74
InternVL3.5-38B	63.92	57.85	61.11	73.47	64.00	56.33	72.53	71.21	55.92	67.20	54.74
o4-mini	73.00	68.92	76.47	74.83	72.00	69.75	87.91	74.09	73.03	71.10	56.84
Doubao-seed-1.6	77.33	75.38	81.37	74.49	78.18	75.26	90.11	76.97	76.32	75.92	68.42

Table 2: Accuracy scores on **Direct Visual-Aided Reasoning (D-VAR)** task upon **VisAidMath**. Meanings of all abbreviations are: ALL → overall accuracy, PLG → plane geometry, SDG → solid geometry, AYG→ analytic geometry, CAL: calculus and functions. Visual Aids Types: AXL → auxiliary line, RTC → rectangular coordinate, THC → rectangular three-dimensional coordinate, PLG → plane geometry graph, SDG → solid geometry graph, FUG → function graph. The highest scores in chunk and in general have been emphasized with purple and green to facilitate comparison respectively.

deterministic answers, we evaluate the correctness of the final answer using Standard Accuracy (ACCU) as a baseline metric. To accurately extract the final answer from model outputs, we follow the approach of Lu et al. (2023) (Lu et al., 2023) and employ GPT-4o-mini as answer extractor, as it demonstrated a high success rate in preliminary experiments with 200 examples. The prompts used to construct the answer extractor are described in detail in section E.5. ACCU is calculated as:

$$\text{ACCU} = \frac{1}{N}\sum_{j=1}^{N} a_j \tag{1}$$

where N is the total number of samples and $a_j \in \{0, 1\}$ is the binary correctness of the final answer for sample j.

Process-Verified Accuracy (PVA) Recognizing that ACCU cannot distinguish valid reasoning from "lucky guesses," we introduce Process-Verified Accuracy (PVA) to act as a strict reliability filter. PVA refines the initial accuracy score by considering a solution valid only if its final answer is correct *and* its reasoning process is devoid of any critical flaws. This is formalized through a binary judgment based on a hard threshold applied to process quality scores. Formally, PVA is defined as:

$$\text{PVA} = \frac{1}{N}\sum_{j=1}^{N} a_j \cdot V_j \tag{2}$$

where V_j represents the binary validity of the reasoning process for sample j, defined as:

$$V_j = \begin{cases} 1 & \text{if } \min_{i \in \mathcal{D}}(S_{i,j}) > T \\ 0 & \text{otherwise} \end{cases} \quad (3)$$

Here, $\mathcal{D} = \{\text{LogiR, ToolF, InfoT, GeneR}\}$ is the set of evaluation dimensions, $S_{i,j}$ is the score (from 1 to 10) for dimension i of sample j, and T is a predefined critical flaw threshold (e.g., $T = 4$). Any score at or below T indicates a fatal error, causing the entire process to be invalidated ($V_j = 0$).

Solution Process Robustness Score (SPRS) The framework culminates in the Solution Process Robustness Score (SPRS), which offers the most granular level of assessment. Distinct from the binary filtering of PVA, SPRS provides a continuous, fine-grained quality score for all correctly answered problems. It quantifies the overall robustness of a solution by multiplicatively aggregating its scores across all process dimensions. This mechanism, reflecting a "short-plank effect," heavily penalizes any 'weak links' in the reasoning chain. It is calculated as:

$$\text{SPRS} = \frac{1}{N} \sum_{j=1}^{N} a_j \cdot \prod_{i \in \mathcal{D}} \left(\frac{S_{i,j}}{10} \right) \quad (4)$$

The gating by a_j ensures that only correctly answered samples contribute to the score. The product $\prod$ over the normalized dimension scores ($S_{i,j}/10$) ensures that even a single low-quality dimension significantly depresses the overall score for that sample, thus rewarding solutions that are consistently strong across all aspects of reasoning.

3.3 Main Results

Initial Performance via Standard Accuracy The complete performance results are presented in Tables 29, 2, and 30, with a summary of leading models in Table 3. On the metric of standard accuracy (ACCU), top-performing models demonstrate high scores. For instance, Doubao-Seed-1.6 achieves a peak ACCU of **81.00%** on the Indirect Visual-aided Reasoning task and **77.33%** on the Direct Visual-aided Reasoning task. While these figures indicate a strong capability for arriving at correct final answers, they do not, in isolation, validate the underlying reasoning processes used to obtain them.

Performance Collapse under Deeper Scrutiny The insufficiency of ACCU as a standalone metric becomes evident when our Funnel Evaluation Framework is applied. As shown in Table 3, a significant and universal decline is observed from ACCU to both Process-Verified Accuracy (PVA) and Solution Process Robustness Score (SPRS). On the Direct Visual-aided Reasoning task, for example, Doubao-Seed-1.6's 77.33% ACCU declines to a PVA of 62.03% and an SPRS of 47.58%. We define this stark discrepancy between apparent correctness and procedural soundness as the **reasoning illusion**. This phenomenon provides powerful evidence that VisAidMath effectively probes deep reasoning deficiencies that are masked by conventional accuracy-only evaluations. A quantitative analysis of this illusion and its implications for the VisAidMath benchmark is the central focus of Section 4.

4 Analysis

Following the discovery of the universal "reasoning illusion," this chapter provides a deep analysis of this phenomenon. We first offer quantitative proof demonstrating how VisAidMath uniquely exposes model deficiencies, and then present a qualitative diagnosis to understand the root causes behind these failures.

4.1 The Reasoning Gap Quantified

Reliability and Robustness Gaps To objectively measure the performance drop from surface accuracy to procedural quality, we define two metrics: the **Reliability Gap** ('ACCU - PVA') and the **Robustness Gap** ('ACCU - SPRS'). The former quantifies the proportion of correct answers derived from flawed processes, while the latter measures the overall decline in solution quality. Figure 4 visualizes these two gaps across our three reasoning tasks.

The analysis reveals a critical finding: the **Direct Visual-aided Reasoning (D-VAR) task induces a dramatically larger gap** in both reliability and robustness compared to the other tasks. This indicates that while models may seem competent on the surface, their reasoning processes are particularly fragile when required to directly engage with visual information. For instance, InternVL3.5-38B on the D-VAR task exhibits a massive 43.7-point Reliability Gap and a 33.2-point Robustness Gap. This provides strong quantitative evidence that the

Model	ACCU	PVA	SPRS	LogiR	ToolF	InfoT	GeneR
Task 1: General Reasoning							
VL-Cogito	48.00	24.00	11.50	5.86	8.81	8.83	7.80
Qwen2.5-VL-72B	53.17	37.39	24.50	7.42	9.22	9.39	8.73
InternVL3.5-38B	62.00	50.59	41.42	8.33	9.33	9.77	9.25
GPT-4.1	59.42	49.03	39.58	8.55	9.43	9.72	9.22
o4-mini	71.92	63.34	55.00	9.26	9.68	9.94	9.66
Doubao-Seed-1.6	78.75	68.13	55.25	9.09	9.72	9.93	9.61
Task 2: Direct Visual-aided Reasoning							
VL-Cogito	49.17	20.20	8.58	5.20	8.50	8.31	6.94
Qwen2.5-VL-72B	52.25	34.79	21.42	7.13	9.18	9.27	8.54
InternVL3.5-38B	63.92	20.20	30.67	7.93	9.23	9.68	9.19
GPT-4.1	62.42	52.34	44.17	8.72	9.44	9.78	9.38
o4-mini	73.00	53.84	37.92	8.29	9.53	9.44	9.23
Doubao-Seed-1.6	77.33	62.03	47.58	8.63	9.64	9.72	9.40
Task 3: Indirect Visual-aided Reasoning							
VL-Cogito	48.67	25.50	12.67	6.02	8.82	8.84	7.89
Qwen2.5-VL-72B	54.67	37.99	25.92	7.36	9.22	9.44	8.67
InternVL3.5-38B	60.00	47.72	38.67	8.24	9.39	9.76	9.26
GPT-4.1	60.50	51.38	44.67	8.72	9.46	9.75	9.32
o4-mini	73.50	65.02	62.08	9.31	9.74	9.94	9.65
Doubao-Seed-1.6	81.00	69.84	59.25	9.06	9.76	9.90	9.56

Table 3: Comprehensive performance evaluation of different models on three reasoning tasks. We assess multiple models on *General Reasoning*, *Direct Visual-aided Reasoning*, and *Indirect Visual-aided Reasoning*. The metrics include **ACCU** (Accuracy, in %) and our proposed **SPRS** (Solution Process Robustness Score). SPRS is composed of four sub-dimensions, each rated on a 0-10 scale: **LogiR** (Logical Rigor), **ToolF** (Tool-Free Feasibility), **InfoT** (Information Traceability), and **GeneR** (Generality of the Method). A key finding is the significant gap between accuracy (ACCU) and process robustness (SPRS) across all models, underscoring that a correct answer does not guarantee a sound and verifiable reasoning process. For each task, the best score for each metric is highlighted in **green**.

core task of VisAidMath is uniquely effective at pressuring models to reveal their underlying reasoning deficiencies.

Diagnosing Failure Patterns The interplay between PVA and SPRS also serves as a powerful diagnostic tool for identifying distinct model failure modes. The relationship between these two metrics is not uniform across models, revealing different behavioral patterns:

- **Case A: Catastrophic Failures (SPRS > PVA).** For models like InternVL3.5-38B on the D-VAR task (PVA: 20.20%, SPRS: 30.67%), the SPRS score is notably higher than the PVA score. This pattern suggests the model frequently makes critical, "all-or-nothing" errors that cause its solutions to be entirely invalidated by the PVA filter.

- **Case B: Systemic Minor Flaws (PVA > SPRS).** In contrast, models like Doubao-Seed-1.6 (PVA: 62.03%, SPRS: 47.58%) exhibit a higher PVA than SPRS. This indicates the model is more adept at avoiding fatal errors, but its procedurally "valid" solutions are often rife with minor inaccuracies, which are penalized by the SPRS, dragging down the overall robustness score.

This ability to distinguish between models prone to catastrophic accidents and those exhibiting systemic sloppiness underscores the diagnostic depth of our framework.

4.2 Qualitative Diagnosis

Evasion of Visual Reasoning A primary cause for the observed reasoning gap is the strong tendency of models to *evade* the intended visual-aided reasoning path. To investigate this, we manually analyzed 200 correctly answered samples from the D-VAR task. As shown in Figure 5a, a staggering majority of solutions relied on non-visual methods.

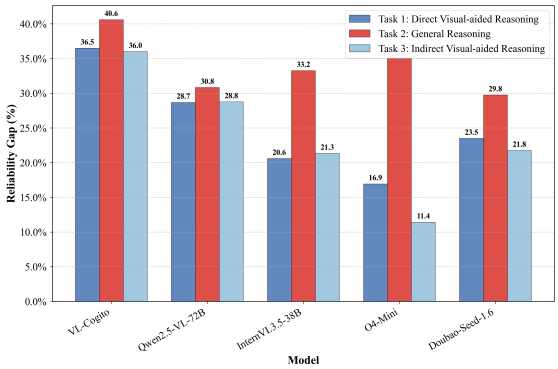

(a) The **Reliability Gap** ('ACCU - PVA') across the three reasoning tasks.

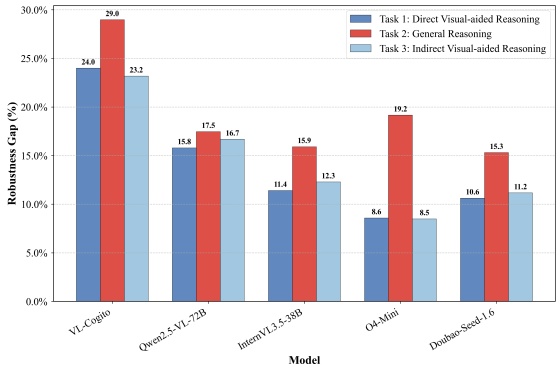

(b) The **Robustness Gap** ('ACCU - SPRS') across the three reasoning tasks.

Figure 4: Performance degradation from surface accuracy (ACCU) to process-level evaluation. The Reliability Gap (a) measures the proportion of correct answers with procedurally invalid reasoning. The Robustness Gap (b) measures the total drop in solution quality. Both gaps are most pronounced in the Direct Visual-aided Reasoning (D-VAR) task, highlighting its unique challenge.

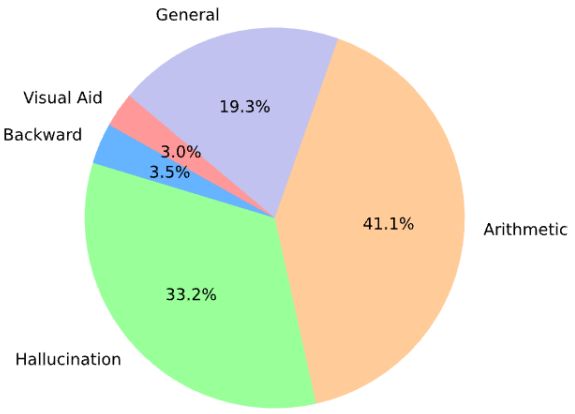

(a) Distribution of reasoning strategies for correctly solved problems. The minimal use of "Visual-Aided" reasoning (3.0%) reveals a strong model tendency to evade the intended solution path.

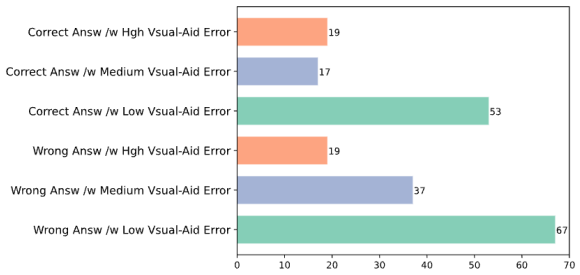

(b) Correlation between visual-aid error severity and final answer correctness. High-severity errors are strongly predictive of an incorrect final answer.

Figure 5: Qualitative diagnosis of the reasoning gap.

Only 3.0% of correct solutions were achieved by generating and using visual aids as intended. The dominant strategies were pure arithmetic (41.1%) or general reasoning that ignored the visual context (19.3%). This indicates a strong tendency for models to bypass the visually-grounded reasoning path in favor of more conventional, text-only strategies. This circumvention of the core task is a key factor explaining how high ACCU scores can mask poor underlying reasoning processes.

The High Cost of Flawed Attempts Furthermore, when models do attempt the visual reasoning path, errors in this intermediate step are often fatal to the final outcome. As demonstrated in Figure 5b, there is a strong correlation between the severity of visual-aid errors and the correctness of the final answer. Solutions with significant visual-aid errors are overwhelmingly more likely to result in an incorrect final answer. This high cost of flawed attempts further explains the significant performance gaps observed in the D-VAR task, as engaging with the task incorrectly is highly detrimental. A more detailed breakdown of these error types can be found in Appendix 28b.

5 Conclusion

Our VisAidMath benchmark reveals that even state-of-the-art models are profoundly deficient in visual-aided mathematical reasoning, failing to connect visual manipulation with logical deduction. This failure exposes a fundamental gap in multi-modal AI and establishes a clear imperative for developing more deeply integrated, visually-grounded models.

Limitations

The limitation of **VisAidMath** is three-folded. First, dataset is restricted to 1200 samples since both collection, annotation and verification of mathematical problems acquire heavy manual work to satisfy dataset principles. Such mathematical problems with visual aids cost more human efforts to understand each segment before judgment. Secondly, deficiency of mainstream machine translation systems in mathematical domain could introduce various translation errors, thus enhancing complexity for problem solving and subsequent evaluation. Thirdly, we cannot conduct comprehensive analysis of visual-aided reasoning with image generation, since current LMMs remain significant deficiency in mathematical image generation. No negative social impact will be provided from our math-centric work, expecting only to enhance further understanding of LLM reasoning.

References

AI Anthropic. 2024. The claude 3 model family: Opus, sonnet, haiku. *Claude-3 Model Card*.

Jinze Bai, Shuai Bai, Shusheng Yang, Shijie Wang, Sinan Tan, Peng Wang, Junyang Lin, Chang Zhou, and Jingren Zhou. 2023. Qwen-vl: A versatile vision-language model for understanding, localization, text reading, and beyond. *arXiv preprint arXiv:2308.12966*, 1(2):3.

Shuai Bai, Keqin Chen, Xuejing Liu, Jialin Wang, Wenbin Ge, Sibo Song, Kai Dang, Peng Wang, Shijie Wang, Jun Tang, et al. 2025. Qwen2. 5-vl technical report. *arXiv preprint arXiv:2502.13923*.

Jiaqi Chen, Tong Li, Jinghui Qin, Pan Lu, Liang Lin, Chongyu Chen, and Xiaodan Liang. 2022. Unigeo: Unifying geometry logical reasoning via reformulating mathematical expression. *arXiv preprint arXiv:2212.02746*.

Xiaoyi Dong, Pan Zhang, Yuhang Zang, Yuhang Cao, Bin Wang, Linke Ouyang, Xilin Wei, Songyang Zhang, Haodong Duan, Maosong Cao, et al. 2024. Internlm-xcomposer2: Mastering free-form text-image composition and comprehension in vision-language large model. *arXiv preprint arXiv:2401.16420*.

Luyu Gao, Aman Madaan, Shuyan Zhou, Uri Alon, Pengfei Liu, Yiming Yang, Jamie Callan, and Graham Neubig. 2023. Pal: Program-aided language models. In *International Conference on Machine Learning*, pages 10764–10799. PMLR.

Google. 2023. https://labelbox.com/product/model/foundry-models/google-gemini-pro-vision/. In *Google*. Google.

Dong Guo, Faming Wu, Feida Zhu, Fuxing Leng, Guang Shi, Haobin Chen, Haoqi Fan, Jian Wang, Jianyu Jiang, Jiawei Wang, et al. 2025. Seed1. 5-vl technical report. *arXiv preprint arXiv:2505.07062*.

Dan Hendrycks, Collin Burns, Saurav Kadavath, Akul Arora, Steven Basart, Eric Tang, Dawn Song, and Jacob Steinhardt. 2021. Measuring mathematical problem solving with the math dataset. *arXiv preprint arXiv:2103.03874*.

Gueyoung Jung, Matti A Hiltunen, Kaustubh R Joshi, Richard D Schlichting, and Calton Pu. 2010. Mistral: Dynamically managing power, performance, and adaptation cost in cloud infrastructures. In *2010 IEEE 30th International Conference on Distributed Computing Systems*, pages 62–73. IEEE.

Takeshi Kojima, Shixiang Shane Gu, Machel Reid, Yutaka Matsuo, and Yusuke Iwasawa. 2022. Large language models are zero-shot reasoners. *Advances in neural information processing systems*, 35:22199–22213.

Aitor Lewkowycz, Anders Andreassen, David Dohan, Ethan Dyer, Henryk Michalewski, Vinay Ramasesh, Ambrose Slone, Cem Anil, Imanol Schlag, Theo Gutman-Solo, et al. 2022. Solving quantitative reasoning problems with language models. *Advances in Neural Information Processing Systems*, 35:3843–3857.

Adam Dahlgren Lindström and Savitha Sam Abraham. 2022. Clevr-math: A dataset for compositional language, visual and mathematical reasoning. *arXiv preprint arXiv:2208.05358*.

Haotian Liu, Chunyuan Li, Yuheng Li, Bo Li, Yuanhan Zhang, Sheng Shen, and Yong Jae Lee. 2024a. Llava-next: Improved reasoning, ocr, and world knowledge.

Haotian Liu, Chunyuan Li, Qingyang Wu, and Yong Jae Lee. 2024b. Visual instruction tuning. *Advances in neural information processing systems*, 36.

Pan Lu, Hritik Bansal, Tony Xia, Jiacheng Liu, Chunyuan Li, Hannaneh Hajishirzi, Hao Cheng, Kai-Wei Chang, Michel Galley, and Jianfeng Gao. 2023. Mathvista: Evaluating mathematical reasoning of foundation models in visual contexts. *arXiv preprint arXiv:2310.02255*.

Pan Lu, Ran Gong, Shibiao Jiang, Liang Qiu, Siyuan Huang, Xiaodan Liang, and Song-Chun Zhu. 2021. Inter-gps: Interpretable geometry problem solving with formal language and symbolic reasoning. *arXiv preprint arXiv:2105.04165*.

Ahmed Masry, Do Xuan Long, Jia Qing Tan, Shafiq Joty, and Enamul Hoque. 2022. Chartqa: A benchmark for question answering about charts with visual and logical reasoning. *arXiv preprint arXiv:2203.10244*.

OpenAI. 2023a. https://openai.com/index/gpt-4v-system-card/. In *OpenAI*. OpenAI.

OpenAI. 2023b. https://platform.openai.com/docs/models/gpt-3-5-turbo. In *OpenAI*. OpenAI.

OpenAI. 2023c. https://platform.openai.com/docs/models/gpt-4. In *OpenAI*. OpenAI.

OpenAI. 2023d. https://platform.openai.com/docs/models/gpt-4.1. In *OpenAI*. OpenAI.

OpenAI. 2023e. https://platform.openai.com/docs/models/o4-mini. In *OpenAI*. OpenAI.

Jack W Rae, Sebastian Borgeaud, Trevor Cai, Katie Millican, Jordan Hoffmann, Francis Song, John Aslanides, Sarah Henderson, Roman Ring, Susannah Young, et al. 2021. Scaling language models: Methods, analysis & insights from training gopher. *arXiv preprint arXiv:2112.11446*.

Hugo Touvron, Louis Martin, Kevin Stone, Peter Albert, Amjad Almahairi, Yasmine Babaei, Nikolay Bashlykov, Soumya Batra, Prajjwal Bhargava, Shruti Bhosale, et al. 2023. Llama 2: Open foundation and fine-tuned chat models. *arXiv preprint arXiv:2307.09288*.

Weiyun Wang, Zhangwei Gao, Lixin Gu, Hengjun Pu, Long Cui, Xingguang Wei, Zhaoyang Liu, Linglin Jing, Shenglong Ye, Jie Shao, et al. 2025. Internvl3. 5: Advancing open-source multimodal models in versatility, reasoning, and efficiency. *arXiv preprint arXiv:2508.18265*.

Thomas Wolf, Lysandre Debut, Victor Sanh, Julien Chaumond, Clement Delangue, Anthony Moi, Pierric Cistac, Tim Rault, Remi Louf, Morgan Funtowicz, Joe Davison, Sam Shleifer, Patrick von Platen, Clara Ma, Yacine Jernite, Julien Plu, Canwen Xu, Teven Le Scao, Sylvain Gugger, Mariama Drame, Quentin Lhoest, and Alexander Rush. 2020. Transformers: State-of-the-art natural language processing. In *Proceedings of the 2020 Conference on Empirical Methods in Natural Language Processing: System Demonstrations*, pages 38–45, Online. Association for Computational Linguistics.

Qinzhuo Wu, Qi Zhang, Jinlan Fu, and Xuan-Jing Huang. 2020. A knowledge-aware sequence-to-tree network for math word problem solving. In *Proceedings of the 2020 conference on empirical methods in natural language processing (EMNLP)*, pages 7137–7146.

Yuhuai Wu, Markus N Rabe, Wenda Li, Jimmy Ba, Roger B Grosse, and Christian Szegedy. 2021. Lime: Learning inductive bias for primitives of mathematical reasoning. In *International Conference on Machine Learning*, pages 11251–11262. PMLR.

Zheng Yuan, Hongyi Yuan, Chuanqi Tan, Wei Wang, and Songfang Huang. 2023. How well do large language models perform in arithmetic tasks? *arXiv preprint arXiv:2304.02015*.

Xiang Yue, Xingwei Qu, Ge Zhang, Yao Fu, Wenhao Huang, Huan Sun, Yu Su, and Wenhu Chen. 2023. Mammoth: Building math generalist models through hybrid instruction tuning. *arXiv preprint arXiv:2309.05653*.

Contents

A Future Direction **11**

B Dataset Analysis **11**
B.1 Metadata 11
B.2 Data Source 11

C Examples for Different Categorizations **13**
C.1 Math Branch 13
C.2 Visual Aid Type 13
C.3 Complexity 13

D Dataset Collection Detail **13**
D.1 Annotation Details 13
D.2 Caption Writing Templates 13
D.3 Dataset Creation Pipeline 13
D.4 Human Annotation Interface . . . 13

E Detail Experiment Settings **24**
E.1 Hyperparameters 24
E.2 Reasoning Prompter 24
E.3 Instruction across Answer Types . 24
E.4 Visual Aid Extraction 24
E.5 Answer Extraction Prompter . . . 24

F More Experimental Results **24**
F.1 Results of other tasks 24
F.2 Quantitative Analysis 24
F.2.1 Performance across Math Branches 24
F.2.2 Performance across Complexities 26
F.2.3 Performance across Visual Aids 26
F.3 N-gram Similarities 29

G In-depth Model Analysis **33**
G.1 General Reasoning Tendency . . . 33
G.2 Visual Aid Inference Capability . 33

H Supplementary Quantitative Analysis **34**

I Related Work **36**

Appendix

A Future Direction

Spatial Capability Despite the predominant emphasis on the construction and fitting of extensive datasets, mainstream works are confined to inference tasks within textual dimension. LLM exhibits exceedingly poor performance in providing visual reasoning step, revealing deficiencies in spatial understanding, imagination, and more other aspects. To address mathematical reasoning with visual-aid inference, future investigation could be directed to specifically enhance LLM's adaptation to visual reasoning tasks, devise new methods for better integration of textual and visual reasoning, or design specific architectures for multimodal reasoning steps inference.

Mathematical Image Generation Preliminary experiments find mainstream models exhibit poor mathematical image generation performance, thus further captioning each mathematical images to explore visual reasoning step inference. Primary model deficiencies fall in: mathematical image caption comprehension, spatial relationships apprehension, lack of numerical precision, significant stylization discrepancies in the images, and more. Generate image drawing code can increase the overall drawing precision, while suffering from plenty of code errors. There lies a long research road in mathematical image generation before fully exploration of textual-visual interconnected inference.

Evaluation Metrics Reasoning non-uniqueness enhances evaluation complexity of visual aids generation. Different viewing angle, relative element size, and styles can alter perceptual features instead of semantic feature. Visual-aid can be captioned by multiple correct expressions with semantic remains stable. Therefore, future evaluation metrics research for visual-aid should be directed toward semantic-based method.

B Dataset Analysis

B.1 Metadata

We list the manually annotated metadata for each sample in Table **??**. "visual context" is optional depending on whether image is provided along with the problem. "choices" is not empty when question form belongs to multiple choices or true/false. "language" stamp the original language of each problem. We also record the Chinese version text before machine translation with "zh_" prefix at the bottom of each data sample.

B.2 Data Source

In accordance with the aforementioned principles, the VisAidMath benchmark has been manually collected and annotated using a diverse and balanced set of data sources. Through an extensive search

Category	Detail
question	Text of mathematical problem
visual context: image path	Relative path of visual context image
visual context: caption	Caption of visual context image
visual aid: image path	Relative path of visual aids image
visual aid: caption	Caption of visual aids image
choices	Options for multiple choice problems
question form	Question form includes: multiple choice, true/false, free form
answer form	Integer, decimal, fraction, and choice (for multiple choice and true/false problems)
answer	Answer of this mathematical problem
metadata: language	Original language of this mathematical problem.
metadata: source	Data source
metadata: math branch	Mathematical branch
metadata: drawing type	type of visual aids

Table 4: Detail metadata for **VisAidMath**

Category	Detail
question	Text of mathematical problem
visual context: image path	Relative path of visual context image
visual context: caption	Caption of visual context image
visual aid: image path	Relative path of visual aids image
visual aid: caption	Caption of visual aids image
choices	Options for multiple choice problems
question form	Question form includes: multiple choice, true/false, free form
answer form	Integer, decimal, fraction, and choice (for multiple choice and true/false problems)
answer	Answer of this mathematical problem
metadata: language	Original language of this mathematical problem.
metadata: source	Data source
metadata: math branch	Mathematical branch
metadata: drawing type	type of visual aids

Table 5: Detail metadata for **VisAidMath**

and careful examination on a case-by-case basis, we discovered that the Chinese community offers a larger pool of mathematical problems with visual aids across various complexity levels and mathematical branches compared to other communities. As a result, we primarily collected data from Chinese sources and subsequently performed machine translation. To ensure formula consistency, we replace LaTeX formulas with placeholders before translation and refill afterward. We also provide human validation of all samples to further ensure translation quality. To ensure a range of difficulty levels, we categorized the data samples based on their sources into the following categories: Easy, Medium and Hard. Additionally, metadata has been included for further in-depth analysis, discuessed in section B.1.

We analyze the problem complexity of 16 data source following three difficulty levels: 1) Easy: Chinese High school entrance examination 2) Medium: Chinese College Entrance Examination 3) High: Chinese Mathematical Olympiad. The complete complexity categorization of each source is listed in 6. Particularly, since "AP Calculus"

consists of both easy and medium level mathematical problems, we consider questions satisfying one of the following conditions as medium level: 1) involve coordinate axes rotation 2) cannot be resolved in one step leveraging Newton-Leibniz formula.

C Examples for Different Categorizations

C.1 Math Branch

As shown in Table **??**, this section presents examples of mathematical problems from different branches: plane geometry, solid geometry, analytic geometry, and calculus. Each example includes a question and visual aids to help illustrate the concepts.

C.2 Visual Aid Type

C.3 Complexity

D Dataset Collection Detail

D.1 Annotation Details

The quality of annotation plays a crucial role in ensuring the reliability of the benchmark, and the annotation of metadata significantly impacts the depth and breadth of analysis. In the annotation process, we instructed the annotators to label various metadata, including the *math category*, *source*, *visual aids' type*, *question form*, *choices*, *answer form*, *answer*, and *language*. Given that the formalization of mathematical problems can vary significantly across different data sources, we specifically asked the annotators to manually extract the question and answer text from the LaTeX file to ensure completeness and accuracy. Following the approach used in MathVista (Lu et al., 2023), we transformed free-form questions without a purely numerical answer into multiple-choice or True/False questions. This deterministic transformation allows for a more robust evaluation. To create precise and comprehensive descriptions of the visual context and visual aids, we provided the annotators with caption writing templates that were designed to simplify the complexity of caption writing. For more details, please refer to section D.2. Four Chinese undergraduate students who majored in STEM during their high school period were carefully selected to form our annotation team. The collectors and annotators were compensated salary aligns with average price in local data crowdsourcing market for each data sample they collected or annotated. Furthermore, a graduate student specializing in mathematics was appointed as the verifier, offering professional annotation guidance, validation, and refinement throughout the process.

D.2 Caption Writing Templates

Mathematical graphs are consists of shapes and elements bound with specific relation or theorem. To reduce manual annotation work and enhance caption consistency, we standardize the caption writing for visual context and visual aids by defining templates for certain visual elements. The annotators should caption image referring to these templates as listed in **??**.

D.3 Dataset Creation Pipeline

The pipeline is shown in the Figure 9.

D.4 Human Annotation Interface

Shown in the Figure 10.

Data Source	Detail
High Textbook	Chinese high school textbook
Middle Practice	Chinese high school practice sheet
AP Easy	AP calculus (categorized into `Easy` category)
Middle Simulate	Chinese middle school simulated examination
AP Middle	AP calculus (categorized into `Medium` category)
High Practice	Chinese high school practice sheet
DSE Final	HKDSE final examination
High Final	Chinese high school final examination
High Simulate	Chinese high school simulated examination
Math Analysis Demidovich Textbook	Demidovich Problems in Mathematical Analysis
Analytic Geometry Lv Textbook	Analytic geometry textbook written by Lingen Lv
CMO Final	Chinese Mathematical Olympiad
CMO Practice	Chinese Mathematical Olympiad practice sheet
AIME Final	American Invitational Mathematics Examination (AIME)
AMC 8 Practice	American Mathematics Competition 8 (AMC 8)
AMC 10 Final	American Mathematics Competition 10 (AMC 10)

Table 6: Detail of data sources

ID: 1114

Question: determine that the sum of the squares of the lengths of the three medians of a triangle is equal to the sum of the squares of the lengths of the three sides $\frac{3}{4}$.

Visual Aids: 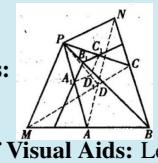

Caption of Visual Aids: Let the three vertices of a triangle be the midpoint of A, B, C, AB , the midpoint of F, AC , the midpoint of E, BC , and the midpoint of D , connecting AD, BE, CF

Table 7: Example of mathematical problems of plane geometry.

ID: 1006

Visual Context: 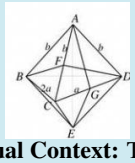

Caption of Visual Context: Two congruent triangles are glued together to obtain a hexahedron with all the dihedral angles equal, and the length of the shortest prong of the hexahedron is 2.

Question: Given that two congruent triangular pheons are glued together to obtain a hexahedron with all the dihedral angles equal, and that the shortest prong of the hexahedron is 2, the distance between the two farthest vertices is

Visual Aids: 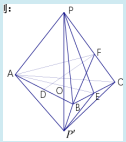

Caption of Visual Aids: Make a plane $BDF \perp$ with edges AC intersecting AC at F

Table 8: Example of mathematical problems of solid geometry.

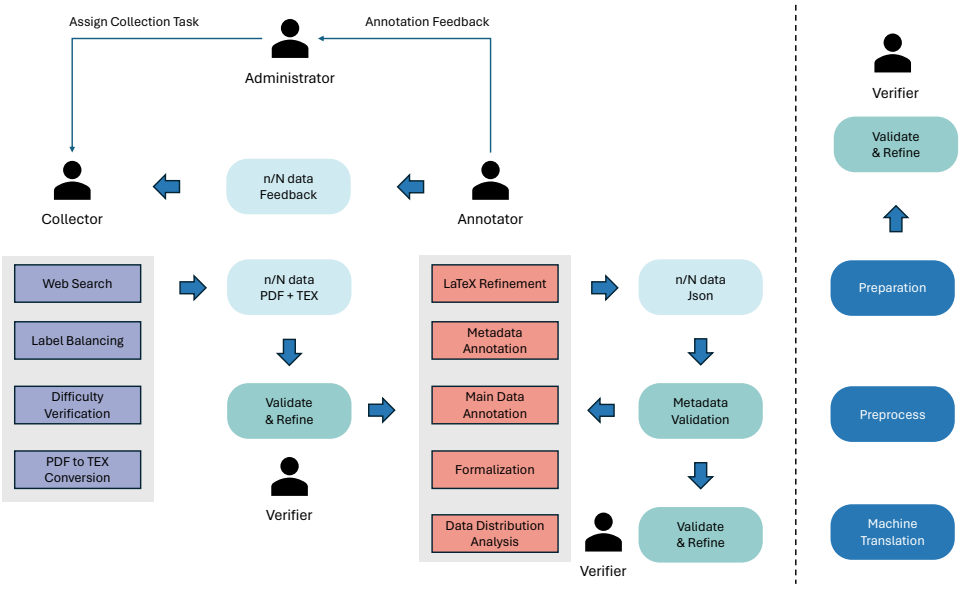

Figure 6: Pipeline invloving data collection, annotation and verification.

ID: 619

Visual Context: 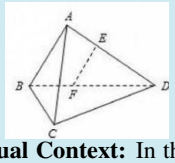

Caption of Visual Context: In the trigonometry $\mathrm{A}-\mathrm{BCD}$, $\mathrm{AB} \perp \mathrm{AD}, \mathrm{BC} \perp \mathrm{BD}$, the plane $\mathrm{ABD} \perp$ the plane BCD, points $\mathrm{E},\ \mathrm{F}(\mathrm{E}$ do not coincide with $\mathrm{A}, \mathrm{D})$ are on the prisms AD, BD and EF BD respectively. $\perp \mathrm{AD}$. EF / $/ Plane$ ABC
Question: In the trigonal pheasant $\mathrm{A}-\mathrm{BCD}$, $\mathrm{AB} \perp \mathrm{AD}, \mathrm{BC} \perp \mathrm{BD}$, plane $\mathrm{ABD} \perp$ plane BCD , points $\mathrm{E},\ \mathrm{F}(\mathrm{E}$ and A, D do not coincide) on the prong AD, BD respectively, and $\mathrm{EF} \perp \mathrm{AD}.\mathrm{EF}//$ plane ABC determine whether $\mathrm{AD} \perp \mathrm{AC}$.

Visual Aids: 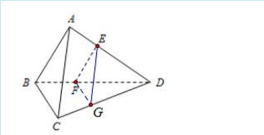

Caption of Visual Aids: Take a point Gon the line segment CD, connect FG, EGso that $\mathrm{FG}//\mathrm{BC}$

Table 9: Example of mathematical problems of analytic geometry.

ID: 939

Question: Can the surface of a container formed by rotating the curve $y = Cx^4$about the vertical axis Oycause the liquid surface to fall uniformly as it flows from the bottom of the container?

Visual Aids: 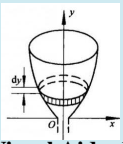

Caption of Visual Aids: In a geometric body obtained by rotating an upward parabola along the xaxis, dxis a line segment parallel to the xaxis, and the volume enclosed by it is drawn

Table 10: Example of mathematical problems of calculus and functions.

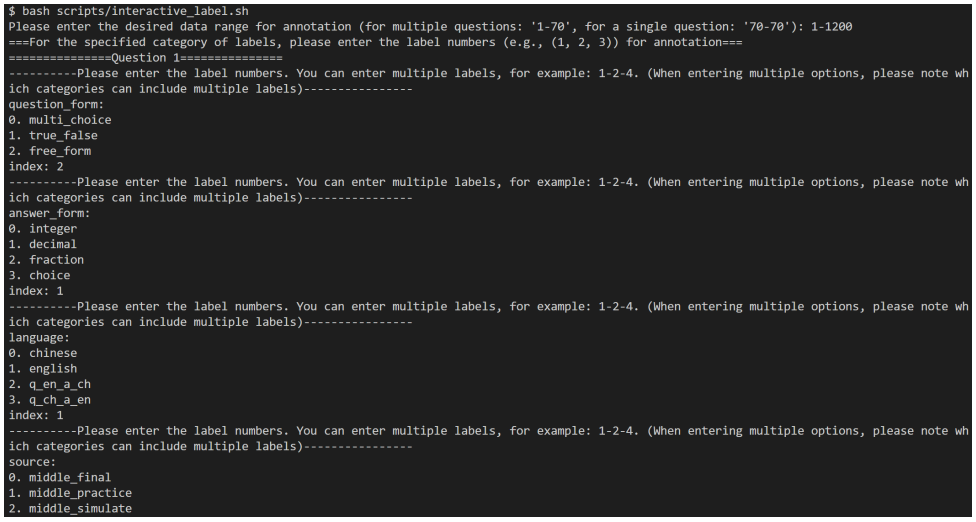

Figure 7: Annotation tool for interactive labeling

ID: 10

Visual Context: 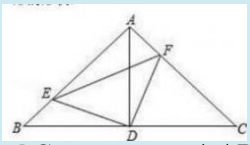

Caption of Visual Context: In Rt $\triangle ABC$, $\triangle BAC = 90^\circ$, point D is the midpoint of BC, points E, F are points on AB, AC respectively, and $ED \perp FD$.

Question: As shown in the figure, in Rt $\triangle ABC$, $\angle BAC = 90^\circ$, the point D is the midpoint of BC , the point E, F is the point on AB, AC , and $ED \perp FD$. Can a triangle be formed with the segment BE, EF, FC as its side? If so, determine the shape of the triangle.

Visual Aids: 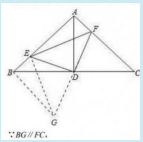

Caption of Visual Aids: Make $BG//FC$, intersect with FD extension line at G , connect EG

Table 11: Example of mathematical problem with auxiliary line as visual aid.

ID: 719

Question: Given that the vector $\overrightarrow{OA}, \overrightarrow{OB}$ satisfies $|\overrightarrow{OA}| = |\overrightarrow{OB}| = 1, \overrightarrow{OA} \perp \overrightarrow{OB}, \overrightarrow{OC} = \lambda\overrightarrow{OA} + \mu\overrightarrow{OB}(\lambda, \mu \in R)$, if M is the midpoint of AB and $|\overrightarrow{MC}| = 1$ then the maximum value of $\lambda + \mu$ is ( )

Choices: A. $1-\sqrt{3}$ B. $1+\sqrt{2}$ C. $\sqrt{5}$ D. $1+\sqrt{3}$ **Visual Aids:** 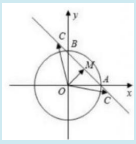

Caption of Visual Aids: Establish a Cartesian coordinate systemDraw the vector $\overrightarrow{OA}, \overrightarrow{OB}$ M is the midpoint of AB

Table 12: Example of mathematical problem with rectangular coordinate system as visual aid.

ID: 1099

Visual Context: 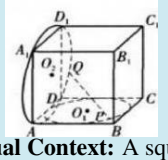

Caption of Visual Context: A square $ABCD - A_1B_1C_1D_1$ has prism length $1, \odot O_1$ is the incircle of the square $ABCD$, $\odot O_2$ is the outer circle of the square ADD_1A_1, and P, Q are the points on $\odot O_1, \odot O_2$ respectively.

Question: As shown in the figure, the prisms of the square $ABCD - A_1B_1C_1D_1$ have the lengths $1, \odot O_1$ as the tangent circle of the square $ABCD$, $\odot O_2$ as the outer circle of the square ADD_1A_1 , and P, Q as the point on $\odot O_1, \odot O_2$. Find the range of the length of PQ .

Visual Aids: 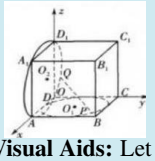

Caption of Visual Aids: Let the origin Oand Dpoints coincide, along DD_1 Establish the Zaxis in the DCdirection, establish the yaxis in the DAdirection, and establish the Xaxis in the DCdirection

Table 13: Example of mathematical problem with rectangular three-dimensional coordinate system as visual aid.

ID: 723

Question: Given that the plane vector $\vec{a}, \vec{b}, \vec{c}$ satisfies the angle between $|\vec{a}| = 1, |\vec{b}| = \sqrt{3}, \vec{a} \cdot \vec{b} = 0, \vec{c} - \vec{a}$ and $\vec{c} - \vec{b}$ is $\frac{\pi}{6}$, then the maximum value of $\vec{c} \cdot (\vec{b} - \vec{a})$ is

Visual Aids: 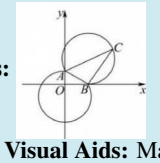

Caption of Visual Aids: Make the tangent between circle o and circle c I_1, I_2, I_3

Table 14: Example of mathematical problem with geometry graph as visual aid.

ID: 220

Visual Context: 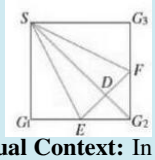

Caption of Visual Context: In the square $SG_1G_2G_3$, E, F are the midpoints of G_1G_2, G_2G_3 respectively, and D is the midpoint of EF, connecting EF, SE, SF, SG_2.

Question: As shown in the figure, in the square $SG_1G_2G_3$, E, F is the midpoint of G_1G_2, G_2G_3 and D is the midpoint of EF respectively. If this square is folded into a tetrahedron along SE, SF and EF so that the three points of G_1, G_2, G_3 coincide, and the point of coincidence is labeled G , then which of the edges of the tetrahedron $SEFG$ are perpendicular to the faces of the tetrahedron?

Visual Aids: 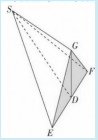

Caption of Visual Aids: Make a four prism S-EFG and unfold it with SG GE GF to form the original square $SG_1G_2G_3$

Table 15: Example of mathematical problem with solid geometry as visual aid.

ID: 394

Question: Through the parabola $C: y^2 = 2px(p\>0)$ The focus of F, as the slope of $2\sqrt{2}$line $l$and parabola Cintersect at two points A, B, If $\overrightarrow{AF} = \lambda\overrightarrow{FB}$, $\lambda = (\quad)$

Visual Aids: 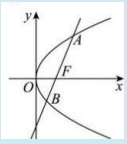

Caption of Visual Aids: Let me draw the parabola $C: y^2 = 2px(p\>0)$, focus F, as the slope of $2\sqrt{2}$line $l$and parabola Cintersect at two points A, B

Table 16: Example of mathematical problem with function graph as visual aid.

ID: 30

Data Source: Chinese Middle School Practice

Visual Context: 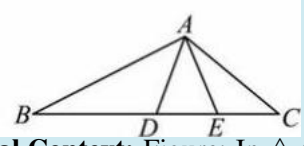

Caption of Visual Context: Figure: In $\triangle ABC$, $BD = DC = AC$, AE is the center line of $\triangle ADC$.

Question: It is known that, as shown in the figure: $\triangle ABC$, $BD = DC = AC, AE$ is the center line of $\triangle ADC$: judge if: $AB = 3AE$.

Visual Aids: 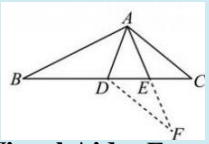

Caption of Visual Aids: Extend AE to F , connect $EF = AE$ to DF

Table 17: Example of mathematical problem classified into "Easy" category

ID: 650

Data Source: HKDSE Examination

Visual Context: 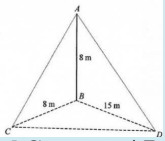

Caption of Visual Context: AB is a vertical pole standing on the horizontal ground BCD, where $\angle CBD = 90^\circ$

Question: In the figure, AB is a vertical pole standing on the horizontal ground BCD, where $\angle CBD = 90^\circ$. If the angle between the plane ACD and the horizontal ground is θ, then $\tan\theta =$

Visual Aids: 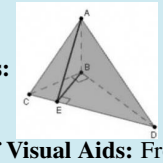

Caption of Visual Aids: From point B to point CD , the perpendicular intersects point CD at point E , connecting AE , BE

Table 18: Example of mathematical problem classified into "Medium" category

ID: 1024

Data Source: Chinese Mathematical Olympiad (CMO)

Visual Context: 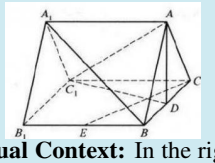

Caption of Visual Context: In the right triangular prism $ABC - A_1B_1C_1$, $AB = AC = 5, D, E$ are the midpoints of BC, BB_1 respectively, and the quadrilateral B_1BCC_1 is a square with side length 6.

Question: As shown in the figure, in the rectangular triangular prism $ABC - A_1B_1C_1$, $AB = AC = 5, D, E$ are the midpoints of BC, BB_1 and the quadrilateral B_1BCC_1 is a square of side 6. determine that: $A_1B//$ is in the plane of AC_1D .

Visual Aids: 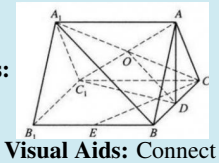

Caption of Visual Aids: Connect A_1C , intersect with AC_1 at O point, connect OD

Table 19: Example of mathematical problem classified into “Hard” category

Category	Detail
Auxiliary Line	1.1 Connect the points a,b to make the line segment 1.2 Connect points a,b and extend them to intersect the CD line at point E. 1.3 Make a vertical line AB through point a.
Rectangular Three-Dimensional Coordinate System	2.1 Establish a three-dimensional rectangular coordinate system with point o as the origin and oa as the x-axis positive direction and ob as the y-axis and oc as the z-axis positive direction.
Rectangular Coordinate System	3.1 Take point o as the origin oa as the x-axis positive direction ob as the y-axis Establish a right-angle coordinate system 3.2 With point o as origin oa as x-axis positive direction y-axis positive direction as x-axis rotated 90 degrees counterclockwise/clockwise
Function Graph	4.1 Draw the $y^2 = ax$ image in the real coordinate system with 0 as the origin. 4.2 Draw the $y^2 = ax$ image in the real coordinate system with 0 as the origin and the y=ax image intersecting at point k in the first quadrant and at point D in the second quadrant.
Riemann integral problem	5.1 Draw the graph of [`function`] function in interval [`interval`] and draw the Riemann integral graph in units of [`unit`] with values on the right/left/middle side.

Table 20: Caption writing templates of various visual aid types for annotators' reference.

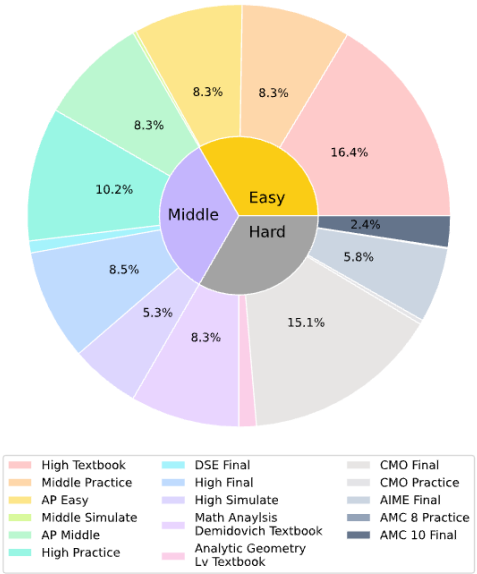

Figure 8: Distribution of data sources and difficulty levels.

E Detail Experiment Settings

E.1 Hyperparameters

We utilize the default inference settings for each LLMs and LMMs in our experiments. Only specific hyperparameters that are necessary to clarify are listed in Table 24 and 25. We conduct open source model inference based on (Wolf et al., 2020). We report a single run score for each experiment.

E.2 Reasoning Prompter

We list the ICL prompts for assigning different models to perform reasoning under six task settings in mathematical domain: 1) CQ2A 2) CQ2VA 3) CQpV2A 4) pCQ2A 5) pCQ2VA 6) pCQpV2A. Task instructions for each task are listed in Table 26. ICL examples can be found at our code open sourced after acceptance.

E.3 Instruction across Answer Types

To facilitate accuracy evaluation, each sample is bound with with non-ambiguous result across integer, fraction, decimal and choice. We define choice as answer type for multiple choice and true/false problems. The specific task instruction for each output answer type is shown in Table 27.

E.4 Visual Aid Extraction

Reasoning prompter instruct models to provide visual aids, reasoning and answer following certain format. We can directly extract visual aids and followup reasoning from output generated by LLM and LMMs with sufficient zero-shot reasoning capability (eg. GPT-4, GPT-4V). However, few weaker models (eg. llama2, LLaVA-Next-Mistral-7B) fail to provide standardized output. We regard these output as both visual-aid and followup reasoning for later answer extraction and similarity evaluation respectively.

E.5 Answer Extraction Prompter

Answer extraction is conducted upon the extracted reasoning text from model output. We provide five ICL examples instructing GPT-4 to extract answer from varied model outputs. Examples are shown in Table 28.

.

F More Experimental Results

More experimental results are in Figure 9.

F.1 Results of other tasks

F.2 Quantitative Analysis

As shown in Figures 10, 11, and 12, the accuracy scores of LMMs and LLMs across math branches show that GPT4V and Gemini-Pro-Vision excel in different tasks with visual aids.

F.2.1 Performance across Math Branches

Figure 10, 11, and 12 illustrate the accuracy scores of LMMs upon three tasks with image input across four math branches. GPT4V outperforms other models in problems within "plane geometry", "analytic geometry", and "calculus and functions" branches. Gemini-Pro-Vision achieves the highest score on solid geometry problems. Notably Claude-3-Sonnet and InternLM-XComposer2-VL both achieves comparable results toward GPT4V in "solid geometry" branch when reason with provided visual-aided, exhibiting robustness and enhanced capabilities in spatial understanding and visual reasoning under "solid geometry". GPT4V underperforms in direct visual-aided reasoning, exhibiting significant deficiency processing implicit visual information. Gemini-Pro-Vision performs better at "analytic geometry" and "calculus and functions" with provided visual aids, demonstrating better understanding of visual context within these mathematical branches.

The accuracy scores of both LLMs and LMMs on three tasks with image caption for visual context across math branches is shown in Figure 13, 14, and 15. In text-only reasoning, GPT4 outperforms other models across most branches and tasks. GPT4V and Gemini-Pro-Vision achieve the highest score at "plane geometry" and "solid geometry" respectively in pCQ2A task. Gemini-Pro-Vision also attains the best score at "solid geometry" branch, manifesting robust visual context utilization within "solid geometry" branch. GPT4V and GPT4 share similar performances over "plane geometry" problems. However, performance of these two models deviates when conduct indirect reasoning. However, GPT-4V achieves significantly lower accuracy on "analytic geometry" branch, demonstrating difficulty for GPT-4V to handle additoinal visual information on "analytic geometry" branch. Gemini-Pro-Vision outperform other models after introduce visual aids into reasoning at "solid geometry" category, indicating better three-dimensional spatial information understanding and processing. Overall, more models perform reasoning better with

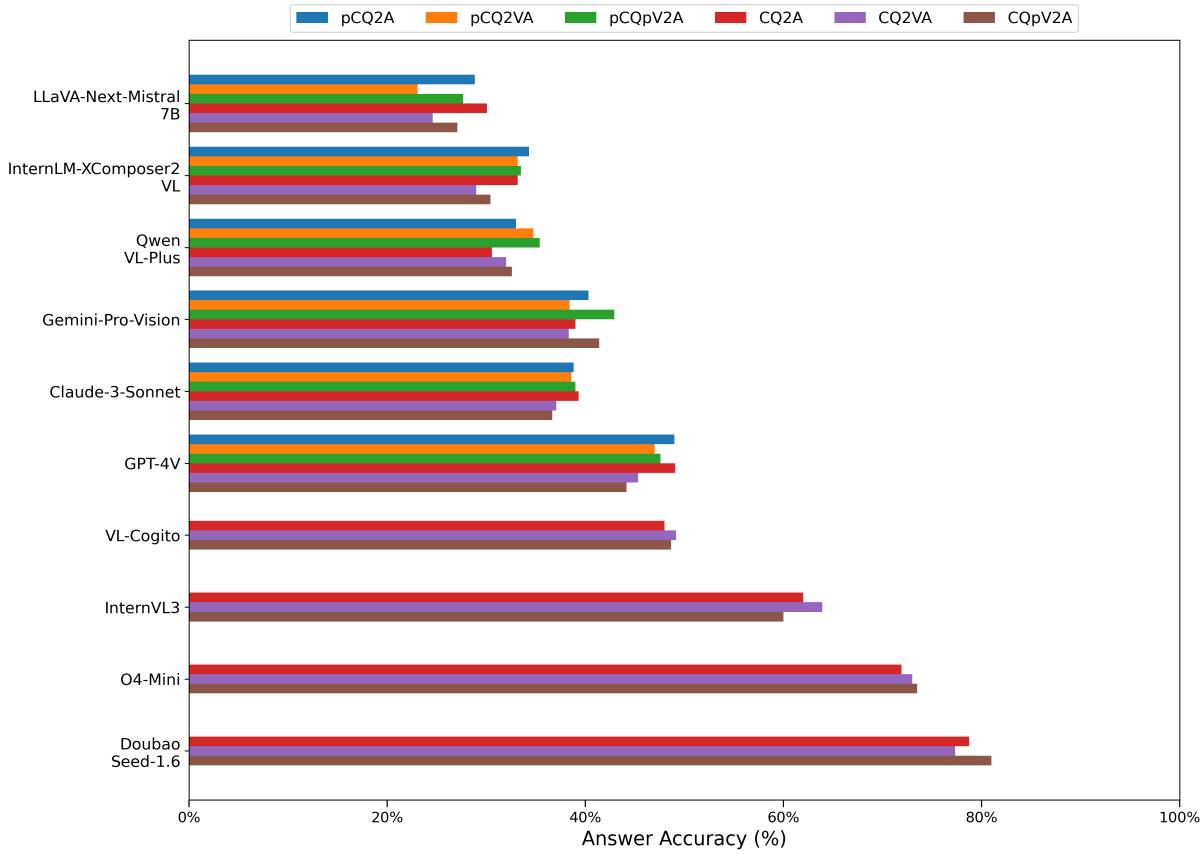

Figure 9: CQ2A is corresponding to GR, CQ2VA is corresponding to D-VAR, and CQpV2A is corresponding to I-VAR.

Visual Context:

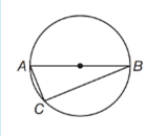

Question: $\overline{AB}$ is a diameter, $AC = 8$ inches, and $BC = 15$ inches. Find the radius of the circle.

GPT4 Reasoning: To solve for the radius of the circle, we can use the fact that triangle ACB is a right triangle because AB is the diameter of the circle (Thales' theorem). Given: • AC=8 inches • BC=15 inches Using the Pythagorean theorem in triangle ACB: AB2=AC2+BC2 Substitute the given values: AB2=82+152=64+225=289 Thus, AB=289=17 Since AB is the diameter, the radius r is half of AB: r=172=8.5 The correct answer is (C) 8.5.

Table 21: An MPS example with visual context from MathVista and reasoning provided by GPT4V.

Visual Context:

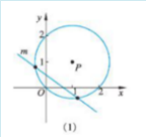

Question: It is known that the line $m : 3x + 4y - 2 = 0$ and the circle $P : x^2 - y^2 - 2x - 2y = 0$. (2) From the graph drawn in (1), determine the relationship between the line m and the circle P. If they intersect, find the length of the chord of the line m intercepted by the circle P. If they are tangent or disjoint, give a proof.

Table 22: An example of using only arithmetic methods to solve mathematical problems

GPT4 Reasoning: Step 1: Solve m for y to find the slope and intercept: ... $3x + 4y - 2 = 0 \Rightarrow y = -\frac{3}{4}x + \frac{1}{2}$.

Step 2: Complete the square for circle P to find its center and radius:$x^2 - 2x + y^2 - 2y = 0 \Rightarrow (x-1)^2 + (y-1)^2 = 2$.

Step 3: Substitute $y = -\frac{3}{4}x + \frac{1}{2}$ into the circle's equation and solve for x.

Step 4: If two points of intersection exist, $A(x_1, y_1)$ and $B(x_2, y_2)$, use the distance formula to find the chord length:

Chord Length $= \sqrt{(x_2 - x_1)^2 + (y_2 - y_1)^2}$.

The final answer will be the length of the chord, provided as an integer in LaTeX format. Let's carry out the calculations to find the result ...

visual aids on "solid geometry" and "analytic geometry" problems, possibly because visual aids in these problems are bound tighter to the reasoning path. In opposite, visual aids within "plane geometry" problems still often leave broad decision space, thus making it harder to utilize the additonnal visual context. Since various problems of "calculus and functions" can often be solved by generic method, most models maintain the highest accuracy in this branch.

F.2.2 Performance across Complexities

F.2.3 Performance across Visual Aids

With Image as input across different visual aids required to generate, the accuracy scores of mainstream LMMs under three tasks are listed in Figure 22, 23, and 24. GPT-4V outperforms other models on problems with visual aids "auxiliary line" and "function graph" across all three tasks. In text-only reasoning task, GPT-4V achieves leading performance in text-only reasoning except for problems with rectangular three-dimensional coordinate system as visual aids. After introduce visual aids, Gemini-Pro-Vision significantly outperform other

Visual Context:

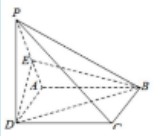

Question: Given that $PD \perp$plane $ABCD$, $ABCD$ is A square, and E is the midpoint of PA, judge :(1) $PC//$plane EBD

Table 23: A successful direct visual-aided reasoning example

GPT4 Constructed Visual Aids: Connect PC and AC, which intersect with BD at point O. Draw a line EO from point E to O.

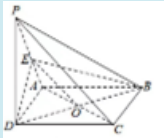

GPT4 Reasoning: Since E is the midpoint of PA and O is the midpoint of diagonal AC of square ABCD:$\because$ EO is parallel to PC (as midlines in a trapezoid).$\because$ PC $\not\subset$ plane EBD and EO $\subset$ plane EBD.$\therefore$ PC is parallel to plane $mathrmEBD$.So the answer is True.

Model	Hyperparameters
GPT3.5	model = `gpt-3.5-turbo`, temperature = 0, max_tokens = 4000
GPT-4	model = `gpt-4-turbo-2024-04-09`, temperature = 0, max_tokens = 4000
Qwen-VL-Plus	model = `qwen-vl-plus`, temperature = 0.7, max_tokens = 4000
Gemini-Pro-Vision	model = `gemini-pro-vision`, temperature = 0.4, max_tokens = 4000
Claude-3-Sonnet	model = `claude-3-sonnet`, temperature = 1, max_tokens = 4000
GPT4V	model = `gpt-4-vision-preview`, temperature = 0, max_tokens = 4000

Table 24: Hyperparameter for close LLMs and LMMs in experiments.

Model	Hyperparameters
Llama2-7B	model = `Llama-2-7b-chat-hf`, precision = bfloat16, temperature = 1.0, max_tokens = 4000
Mistral-7b-Instruct-v0.2	model = `mistral-7b-instruct-v0.2`, precision = bfloat16, temperature = 1.0, max_tokens = 4000
LLaVA-Next-Mistral-7B	model = `llava-v1.6-mistral-7b-hf`, precision = float16, temperature = 1.0, max_tokens = 4000
InternLM-XComposer2-VL	model = `internlm-xcomposer2-vl-7b`, precision = float16, temperature = 1.0, max_tokens = 4000

Table 25: Hyperparameter for open LLMs and LMMs in experiments.

Answer Type	With Visual Context
CQ2A	Please read the following math problem and the related image. After that,
CQ2VA	Please read the following math problem and the related image, then conceive the additional mathematical diagram or visual aid upon provided image to help illustrate the problem, clarify the problem or assist in finding solution. The drawing shape includes auxiliary line, plane geometry graph, solid geometry graph, function graph, plane coordinate and three-dimensional coordinate. These additional drawings can enhance understanding of the problem and potentially find new insights or approaches to solving it. Write drawing description of these additional diagram in text, and express math formula with tex gramma. After that, reason based on the drawing description,
CQpV2A	Please read the following math problem and the related image. Read the provided drawing description of additional mathematical diagram or visual aid upon provided image in latex format, which helps illustrate the problem, clarify the problem or assist in finding solution. The drawing shape includes auxiliary line, plane geometry graph, solid geometry graph, function graph, plane coordinate and three-dimensional coordinate. These additional drawings can enhance understanding of the problem and potentially find new insights or approaches to solving it. After that, based on the drawing description,
pCQ2A	Please read the following math problem and captions of related visual context. After that,
pCQ2VA	Please read the following math problem and captions of related visual context, then conceive the additional mathematical diagram or visual aid upon provided image to help illustrate the problem, clarify the problem or assist in finding solution. The drawing shape includes auxiliary line, plane geometry graph, solid geometry graph, function graph, plane coordinate and three-dimensional coordinate. These additional drawings can enhance understanding of the problem and potentially find new insights or approaches to solving it. Write drawing description of these additional diagram in text, and express math formula with tex gramma. After that, reason based on the drawing description,
pCQpV2A	Please read the following math problem and captions of related visual context. Read the provided drawing description of additional mathematical diagram or visual aid upon provided image in latex format, which helps illustrate the problem, clarify the problem or assist in finding solution. The drawing shape includes auxiliary line, plane geometry graph, solid geometry graph, function graph, plane coordinate and three-dimensional coordinate. These additional drawings can enhance understanding of the problem and potentially find new insights or approaches to solving it. After that, based on the drawing description,

Table 26: Instructions for different mathematical problem solving tasks with visual context inside input.

models on problems with solid geometry graph and three-dimensional rectangular coordinate system as visual aids. Gemini-Pro-Vision also achieves comparable result to GPT-4 in problem solving provided with auxiliary line. Comparing generated and provided visual-aids, overall average accuracy are enhanced saliently on "auxiliary line", "plane coordinate system", and "function graph", exhibiting higher sensitivity in reasoning towards these visual aids.

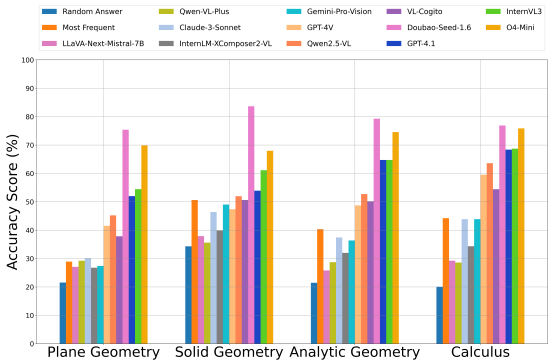

Figure 10: Accuracies of LLMs and LMMs upon CQ2A (General Text-Only Reasoning) task across math branches.

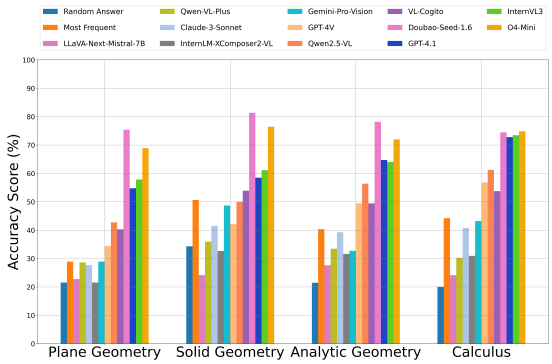

Figure 11: Accuracies of LLMs and LMMs upon CQ2VA (Direct Visual-Aided Reasoning) task across math branches.

Answer Type	Task Instruction
Integer	Answer the question requiring a integer answer in latex format and provide the final value at the end (e.g., -1, 0, 1, 2, 3).
Decimal	Aswer the question requiring a decimal answer in latex format and provide the final value at the end. Make sure the decimal answer is a floating-point number with three decimal place (e.g., 1.234, 2.345, 3.456).
Fraction	Answer the question requiring an fraction answer in latex format and provide the final value at the end. Make sure the fraction answer use '/' as fraction bar and both numerator and denominator are integers (e.g., 1/2, 2/3, 3/4).
Choice (Multiple-Choice)	Answer the question in latex format and provide the correct option at the end. Make sure the option answer can only be single capital letter (e.g., A, B, C, D).
Choice (True/False)	Answer the question in latex format and provide the correct option at the end. Make sure the option answer can only be word 'True' or 'False'.

Table 27: Instructions for mathematical problem solving toward different answer types.

Figure 25, 26, and 27 demonstrate accuracy scores of LLMs and LMMs on three tasks with image caption as input across visual aids. GPT-4 achieves outstanding scores compared to other models. With golden visual aids provided, GPT-4V attains higher accuracy on problem with "solid geometry graph" as visual aids, and Gemini-Pro-Vision well-perform on reasoning with aided "rectangular three-dimensional coordinate system". Overall scores on "plane geometry graph" exhibit substantial difficulty to employ implicit or explicit information within plane geometry graphs.

F.3 N-gram Similarities

We report three n-gram similarities in experiments to fine-grained reveal model capability. For clarity, we first define **hAid** as the generated visual aids from visual-aided generation task. **tAid** is defined as the golden visual aids. **dReas** demonstrates the direct reasoning output from general reasoning task. The three similarity scores include 1) $S_{hAid-dReas}$: overall n-gram similarity between **hAid** and **dReas** 2) $S_{hAid-tAid}$: target-only n-gram similarity between **hAid** and **tAid** 3) $S_{dReas-tAid}$ target-only n-gram similarity between **dReas** and **tAid**. To

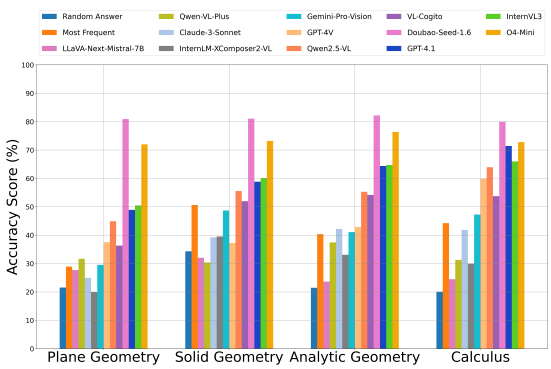

Figure 12: Accuracies of LLMs and LMMs upon CQpV2A (Indirect Reasoning) task across math branches.

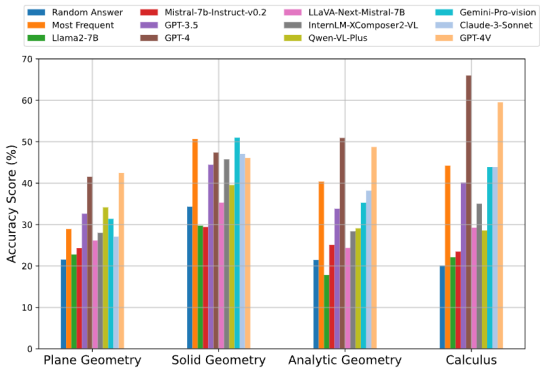

Figure 13: Accuracies of LLMs and LMMs upon pCQ2A (General Text-Only Reasoning) task across math branches.

Element	Prompt
Example 1	**Instruction:** Answer the question requiring a integer answer and provide the final value at the end (e.g., -1, 0, 1, 2, 3). **Question:** Acute Angle $\triangle ABC, BE$vertical ACat E, CDvertical ABat D, given acute Angle $\triangle ABC, BE$vertical ACat E, BCD vertical Ain D, BC = 25, CE = 7, BD = 15, BE, CDto H, connection DE, DEfor circle diameter, and ACto another F, Then the length of AF is **Model response:** Connect DF, then $\angle$DFE = $\angle$BEC = 90°, so DF//BE. In Rt $\triangle$BEC, BC $= 25,$CE $= 7$, so BE $= 24, \cos\angle$ACB $= \frac{7}{25}$, $\sin\angle ACB = \frac{24}{25}$, in Rt $\triangle BCD$, $BC = 25, BD = 15$, so $\cos\angle ABC = \frac{3}{5}, \sin\angle ABC = \frac{4}{5}$. So $\sin A = \sin(\angle ABC + \angle ACB) = \sin\angle ABC\cos\angle ACB + \cos\angle ABC\sin\angle ACB = \frac{4}{5}$, in Rt $\triangle ABE$, sin $A = \frac{BE}{AB} = \frac{24}{AB} = \frac{4}{5}$, we get $AB = 30$, and $BD = 15$, so the point D is the midpoint of AB, and DF is the median of $\triangle ABE$, so $AF = \frac{1}{2}AE = \frac{1}{2}\sqrt{30^2 - 24^2} = 9$. So the final answer is 9 **Extracted answer: 9**
Example 2	**Instruction:** Answer the question requiring a decimal answer and provide the final value at the end. Make sure the decimal answer is a floating-point number with three decimal place (e.g., 1.234, 2.345, 3.456) **Question:** In a right angle $\triangle ABC$, $\angle DAC = 45^\circ, AD = 13, AB = 12$. Calculate the length of CD. **Model response:** Let $DE = x$, then $CE = AE = 13{+}x$, $\frac{12}{13+x} = \frac{5}{x}$ $x = \frac{65}{7}$, $DE = \frac{65}{7}$ $CE = \frac{156}{7}$, $CD = sqrtDE^3 + CE^2 = \frac{169}{7} = 24.1$ **Extracted answer: 24.143**
Example 3	**Instruction:** Answer the question requiring an fraction answer and provide the final value at the end. Make sure the fraction answer use '/' as fraction bar and both numerator and denominator are integers (e.g., 1/2, 2/3, 3/4). **Question:** Linear $x + y = \sqrt{3}$a and round $x^+y^22 = a^2 + (a-1)^2$intersect at point of a,B, $O$is the origin of coordinates, if $triangleisaOB$is triangle, the real value of a **Model response:** From the question, the radius of the circle $r = \sqrt{a^2 + (a-1)^2}$; the distance from the centre of the circle to the line $x + y - \sqrt{3}a = 0$ $d = \frac{\lvert\sqrt{3}a\rvert}{\sqrt{2}}$; because $\triangle AOB$ is a positive triangle, so $d = \frac{\sqrt{3}}{2}r$, i.e. $\frac{\lvert\sqrt{3}a\rvert}{\sqrt{2}} = \frac{\sqrt{3}}{2}\sqrt{a^2 + (a-1)^2}$, which solves $a = \frac{1}{2}$ **Extracted answer: 1/2**

Table 28: 3 ICL examples leveraged to prompt GPT-4 for answer extraction. Full 5 examples will be listed in code open sourced after acceptance.

attain these similarity scores, we first need to count each n-gram size for specific text, g_n represents n-gram chunck:

$$NG = \{Count(g_1), Count(g_2), ..., Count(g_m)\} \tag{5}$$

NG_{clip} calculates the intersecton part of NG_i and NG_j, demonstrating explicit n-gram matches. NG_{base} exhibits essential n-grams to be matched, target-only similarity select NG_i as NG_{base} to emphasize match of target n-grams, while overall similarity leverage union of NG_i and NG_j as the denominator for similarity calculation.

$$NG_{\text{clip}} = NG_i \cap NG_j \tag{6}$$

$$NG_{\text{base}} = \begin{cases} NG_i & \text{if target-only simi} \\ NG_i \cup NG_j & \text{if overall simi} \end{cases} \tag{7}$$

Then,

$$[h]S = \frac{|NG_{\text{clip}}|}{|NG_{\text{base}}|} \tag{8}$$

Qualitative results **??** have shown the best per-

Table 29: Accuracy scores on **General Reasoning task (GR)** task upon **VisAidMath**. Meanings of all abbreviations are listed below. ALL → overall accuracy. For Mathematical Branch: PLG → plane geometry, SDG → solid geometry, AYG→ analytic geometry, CAL: calculus and functions. Visual Aids Types: AXL → auxiliary line, RTC → rectangular coordinate, THC → rectangular three-dimensional coordinate, PLG → plane geometry graph, SDG → solid geometry graph, FUG → function graph. The highest scores in chunk and in general have been emphasized with purple and green to facilitate comparison respectively.

Model	ALL	PLG	SDG	AYG	CAL	AXL	RTC	THC	PLG	SDG	FUG
Heuristics Baselines											
Random Answer	24.42	21.54	34.31	21.45	20.07	24.44	20.87	35.16	10.53	32.89	21.50
Frequent Answer	40.83	28.92	50.65	40.36	44.22	32.79	47.25	74.73	20.00	47.73	44.53
Large Language Models (LLMs): Text-Only Input											
Llama2-7B	23.25	22.77	29.74	17.82	22.11	22.80	19.72	28.57	8.42	28.29	21.11
Mistral-7b-Instruct-v0.2	25.58	24.31	29.41	25.09	23.47	24.59	25.46	25.27	6.32	26.32	25.91
GPT3.5	37.75	32.62	44.44	33.82	40.14	37.85	38.30	40.66	17.89	43.42	38.20
GPT4	51.17	41.54	47.39	50.91	65.99	45.45	55.73	59.34	22.11	49.34	61.80
Large Multimodal Models (LMMs): Text-Only Input											
LLaVA-Next-Mistral-7B	28.83	26.15	35.29	24.36	29.25	27.72	28.67	30.77	10.53	35.53	28.79
InternLM-XComposer2-VL	34.33	28.00	45.75	28.36	35.03	32.64	33.49	53.85	13.68	36.18	33.40
Qwen-VL-Plus	33.00	34.15	39.54	29.09	28.57	34.87	30.05	34.07	13.68	43.42	30.52
Gemini-Pro-Vision	40.33	31.38	50.98	35.27	43.88	36.66	41.28	53.85	17.89	49.34	41.84
Claude-3-Sonnet	38.83	27.08	47.06	38.18	43.88	33.38	39.68	57.14	16.84	48.03	42.80
GPT4V	49.00	42.46	46.08	48.73	59.52	43.82	52.75	52.75	22.11	50.00	57.58
Large Multimodal Models (LMMs): Multimodal Input											
LLaVA-Next-Mistral-7B	30.08	27.08	37.91	25.82	29.25	28.32	29.13	41.76	9.47	34.87	28.98
InternLM-XComposer2-VL	33.17	26.77	39.87	32.00	34.35	30.85	32.80	43.96	11.58	36.84	34.93
Qwen-VL-Plus	30.58	29.23	35.62	28.73	28.57	31.15	29.82	27.47	13.68	41.45	30.52
Gemini-Pro-Vision	39.00	27.38	49.02	36.36	43.88	35.32	40.37	52.75	14.74	48.68	42.03
Claude-3-Sonnet	39.33	30.15	46.41	37.45	43.88	34.72	38.99	56.04	16.84	47.37	42.42
GPT4V	49.08	41.54	47.39	48.73	59.52	43.82	53.21	51.65	24.21	51.97	57.97
VL-Cogito	49.17	40.31	53.92	53.74	49.45	45.31	53.85	52.40	55.26	50.23	20.00
Qwen2.5-VL-72B	52.25	42.77	50.00	61.22	56.36	45.01	50.55	62.38	53.95	58.49	23.16
InternVL3.5-38B	63.92	57.85	61.11	73.47	64.00	56.33	72.53	71.21	55.92	67.20	54.74
GPT-4.1	62.42	54.77	58.50	72.79	64.73	56.93	72.53	70.25	56.58	66.51	54.74
o4-mini	73.00	68.92	76.47	74.83	72.00	69.75	87.91	74.09	73.03	71.10	56.84
Doubao-Seed-1.6	77.33	75.38	81.37	74.49	78.18	75.26	90.11	76.97	76.32	75.92	68.42

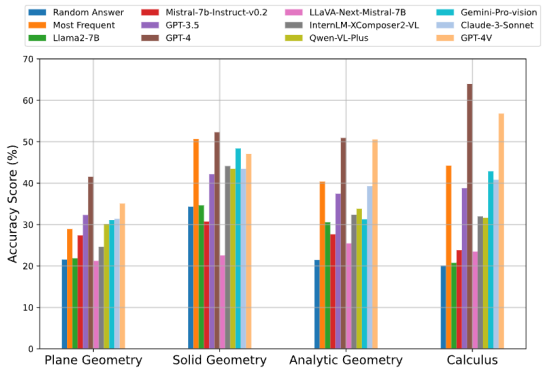

Figure 14: Accuracies of LLMs and LMMs upon pCQ2VA (Direct Visual-Aided Reasoning) task across math branches.

forming GPT4 seldom generates visual aids to assist problem solving, which also confirms with

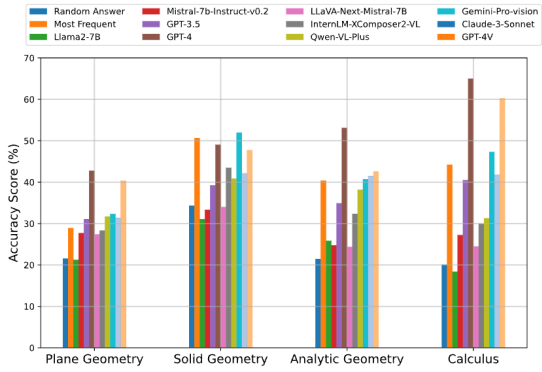

Figure 15: Accuracies of LLMs and LMMs upon pCQpV2A (Indirect Reasoning) task across math branches.

Table 30: Accuracy scores on **Indirect Visual-Aided Reasoning (I-VAR)** task upon **VisAidMath**. Meanings of all abbreviations are listed below. ALL → overall accuracy. For Mathematical Branch: PLG → plane geometry, SDG → solid geometry, AYG→ analytic geometry, CAL: calculus and functions. Visual Aids Types: AXL → auxiliary line, RTC → rectangular coordinate, THC → rectangular three-dimensional coordinate, PLG → plane geometry graph, SDG → solid geometry graph, FUG → function graph. The highest scores in chunk and in general have been emphasized with purple and green to facilitate comparison respectively.

Model	ALL	PLG	SDG	AYG	CAL	AXL	RTC	THC	PLG	SDG	FUG
Heuristics Baselines											
Random Answer	24.42	21.54	34.31	21.45	20.07	24.44	20.87	35.16	10.53	32.89	21.50
Frequent Answer	40.83	28.92	50.65	40.36	44.22	32.79	47.25	74.73	20.00	47.73	44.53
Large Language Models (LLMs): Text-Only Input											
Llama2-7B	24.08	21.23	31.05	25.82	18.37	25.04	22.71	31.87	7.37	30.26	22.46
Mistral-7b-Instruct-v0.2	28.33	27.69	33.33	24.73	27.21	27.72	27.29	34.07	14.74	32.89	27.26
GPT3.5	36.33	31.08	39.22	34.91	40.48	33.08	37.84	50.55	14.74	39.47	39.73
GPT4	52.17	42.77	49.02	53.09	64.97	46.94	57.11	54.95	20.00	52.63	62.76
Large Multimodal Models (LMMs): Text-Only Input											
LLaVA-Next-Mistral-7B	27.67	27.38	33.99	24.36	24.49	27.42	25.00	29.67	11.58	33.55	25.91
InternLM-XComposer2-VL	33.50	28.31	43.46	32.36	29.93	33.68	32.80	49.45	13.68	41.45	31.86
Qwen-VL-Plus	35.42	31.69	40.85	38.18	31.29	36.51	39.22	40.66	15.79	39.47	34.93
Gemini-Pro-Vision	42.92	32.31	51.96	40.73	47.28	39.79	43.35	57.14	17.89	47.37	45.87
Claude-3-Sonnet	39.00	31.38	42.16	41.45	41.84	35.92	40.14	46.15	17.89	42.11	43.19
GPT4V	47.58	40.31	47.71	42.55	60.20	42.32	47.94	50.55	21.05	55.26	53.93
Large Multimodal Models (LMMs): Multimodal Input											
LLaVA-Next-Mistral-7B	27.08	27.69	32.03	23.64	24.49	27.42	24.31	26.37	11.58	32.89	25.72
InternLM-XComposer2-VL	30.42	20.00	39.54	33.09	29.93	26.97	31.88	40.66	10.53	34.87	32.25
Qwen-VL-Plus	32.58	31.69	30.39	37.45	31.29	33.23	38.99	25.27	16.84	37.50	34.55
Gemini-Pro-Vision	41.42	29.54	48.69	41.09	47.28	37.85	43.81	45.05	14.74	48.03	46.07
Claude-3-Sonnet	36.67	24.92	39.22	42.18	41.84	32.04	40.37	41.76	14.74	43.42	43.76
GPT4V	44.17	37.54	37.25	42.91	59.86	38.60	47.25	36.26	17.89	48.03	53.74
VL-Cogito	48.67	36.31	51.96	53.74	54.18	44.86	47.25	54.89	51.32	50.46	16.84
Qwen2.5-VL-72B	54.67	44.92	55.56	63.95	55.27	47.99	56.04	62.76	54.61	58.03	22.11
InternVL3.5-38B	60.00	50.46	60.13	65.99	64.73	55.44	64.84	66.41	59.87	62.39	34.74
GPT-4.1	60.50	48.92	58.82	71.43	64.36	52.01	75.82	69.48	59.21	68.35	46.32
o4-mini	73.50	72.00	73.20	72.79	76.36	70.34	78.02	75.43	73.03	74.08	70.53
Doubao-Seed-1.6	81.00	80.92	81.05	79.93	82.18	78.84	86.81	81.19	78.95	80.28	75.79

quantitative results in Table 31. Since models achieve low $S_{dReas-tAid}$ and tend to solve mathematical problems without visual aids, it becomes necessary to generate visual aids far from **dReas**

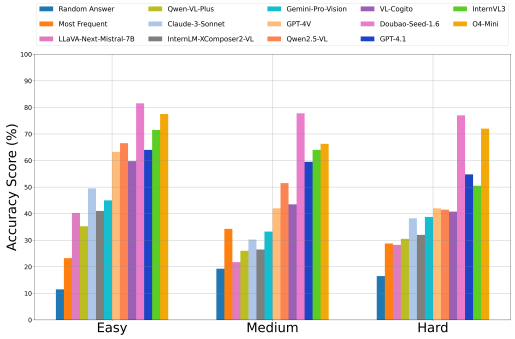

Figure 16: Accuracies of LLMs and LMMs upon CQ2A (General Text-Only Reasoning) task across complexity levels.

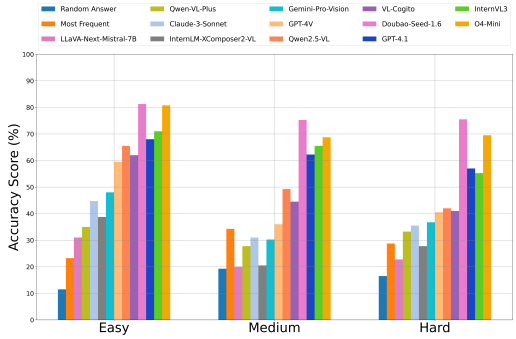

Figure 17: Accuracies of LLMs and LMMs upon CQ2VA (Direct Visual-Aided Reasoning) task across complexity levels.

in direct visual-aided reasoning task. Model with higher $S_{hAid-dReas}$ can easily fail in visual aids inference.

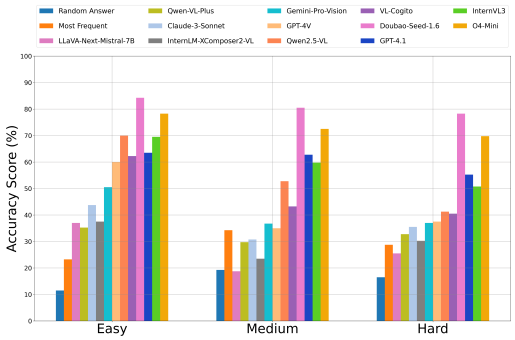

Figure 18: Accuracies of LLMs and LMMs upon CQpV2A (Indirect Reasoning) task across complexity levels.

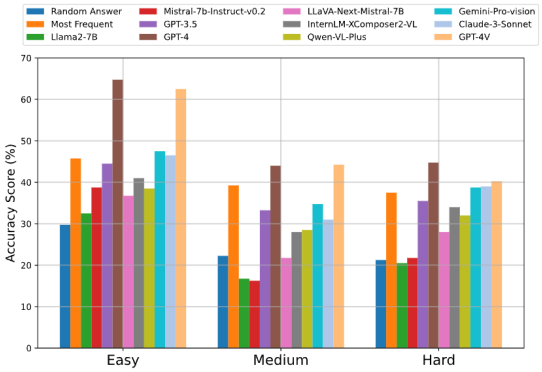

Figure 19: Accuracies of LLMs and LMMs upon pCQ2A (General Text-Only Reasoning) task across complexity levels.

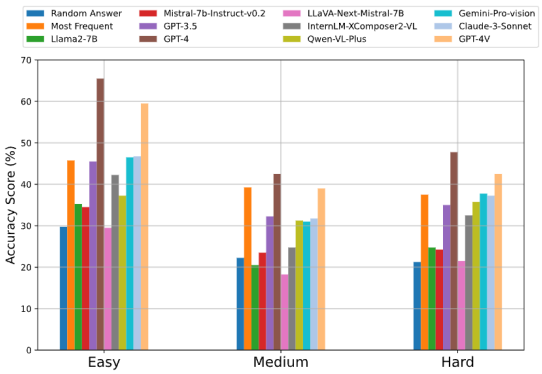

Figure 20: Accuracies of LLMs and LMMs upon pCQ2VA (Direct Visual-Aided Reasoning) task across complexity levels.

G In-depth Model Analysis

G.1 General Reasoning Tendency

G.2 Visual Aid Inference Capability

As shown in Tables 38 and 39, GPT4V demonstrates varying performance in generating visual aids, both correctly and incorrectly.

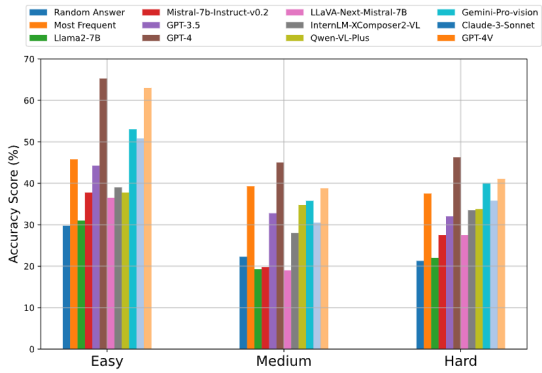

Figure 21: Accuracies of LLMs and LMMs upon pCQpV2A (Indirect Reasoning) task across complexity levels.

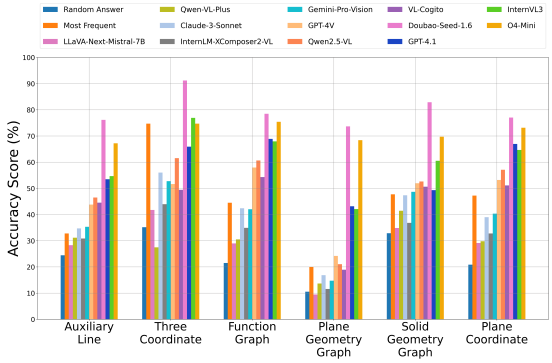

Figure 22: Accuracies of LLMs and LMMs upon CQ2A (General Text-Only Reasoning) task across visual aids.

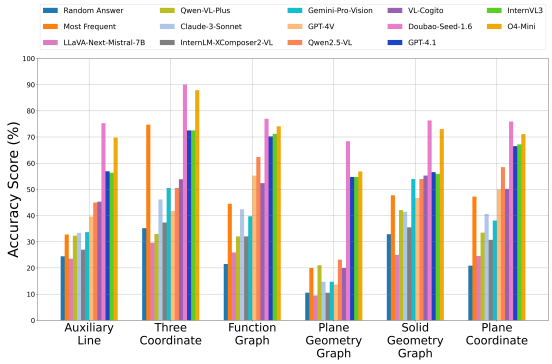

Figure 23: Accuracies of LLMs and LMMs upon CQ2VA (Direct Visual-Aided Reasoning) task across visual aids.

H Supplementary Quantitative Analysis

As shown in Figure 28a and Figure 5b, we analyze reasoning patterns, hallucination correlation, and failure cases of visual-aid generation.

Reasoning Pattern We evaluate only the model outputs with correct answers, examining how GPT4V responds to questions without being instructed to generate visual aids as an intermediate step. We found that GPT4V did not prefer generating visual aids to simplify reasoning complexity. Expect for generating answers due to hallucinations (33.2%), the model searches for problem-solving chains based on visual-irrelevant logic, such as reasoning with pure arithmetic calculations and backward reasoning. An example of solving the problem with pure arithmetic calculation can be found in General Response.

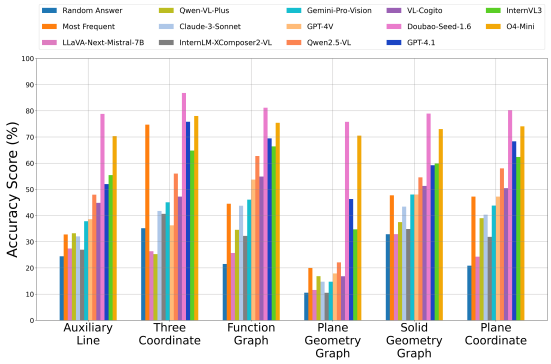

Figure 24: Accuracies of LLMs and LMMs upon CQpV2A (Indirect Reasoning) task across visual aids.

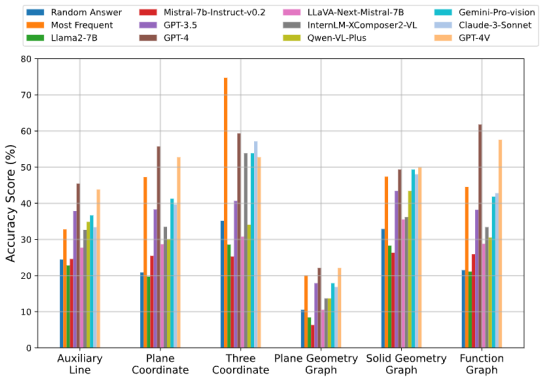

Figure 25: Accuracies of LLMs and LMMs upon pCQ2A (General Text-Only Reasoning) task across visual aids.

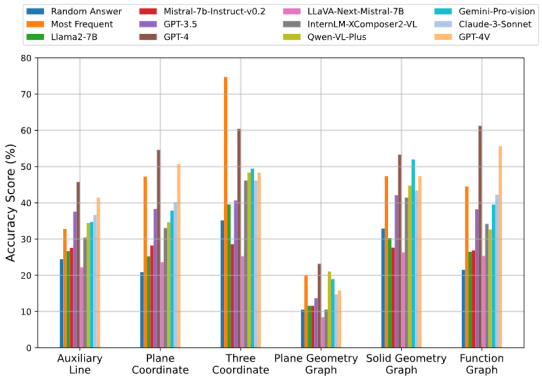

Figure 26: Accuracies of LLMs and LMMs upon pCQ2VA (Direct Visual-Aided Reasoning) task across visual aids.

Model	$S_{hAid-dReas}$	$S_{hAid-tAid}$	$S_{dReas-tAid}$
Large Language Models (LLMs): Text-Only Input			
Llama2-7B	14.73	5.26	3.04
Mistral-7b-Instruct-v0.2	57.21	5.84	4.88
GPT3.5	10.13	4.36	4.29
GPT4	2.37	4.21	3.47
Large Multimodal Models (LMMs): Text-Only Input			
LLaVA-Next-Mistral-7B	29.59	1.96	4.09
InternLM-XComposer2-VL	76.02	4.88	4.84
Qwen-VL-Plus	11.03	1.89	0.85
GeminiPro-vision	7.35	5.37	3.11
Claude-3-Sonnet	2.37	4.66	2.93
GPT4V	1.52	4.03	3.00
Large Multimodal Models (LMMs): Multimodal Input			
LLaVA-Next-Mistral-7B	37.43	1.99	4.04
InternLM-XComposer2-VL	61.43	4.82	4.73
Qwen-VL-Plus	13.71	1.97	0.95
GeminiPro-vision	6.93	5.48	3.08
Claude-3-Sonnet	2.26	4.61	2.95
GPT4V	1.91	3.98	3.03

Table 31: Three types of similarity scores reported across different modles and modalities.

Failure Analysis of Visual Aids Generation We investigated the causes of poorly generated visual aids in the CQ2VA task (i.e., generating visual aids before reasoning). Based on the analysis results, we provide potential research direction for improving the quality of visual aid generation in section A.

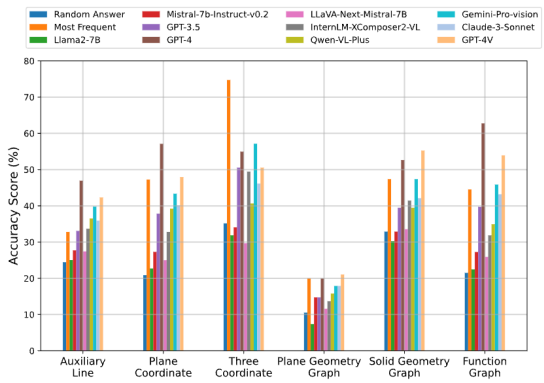

Figure 27: Accuracies of LLMs and LMMs upon pCQpV2A (Indirect Reasoning) task across visual aids.

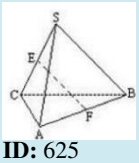

ID: 625

Question: As shown in the figure, the lateral prongs of the square triangular pheasant $SABC$ are equal to the lengths of the sides of the base, and if E, F is the midpoint of SC, AB , then the angle between EF and SA is equal to ( ).

Choices: A. 90° B. 60° C. 45° D. 30°

Table 32: Example of GPT4V solve mathematical problem by creating visual aids to reveal implicit visual information without instructed.

Reasoning: Connect SE and SF, $\because E, F$ are midpoints of SC, AB respectively, and given that $SABC$ is a square triangular pheasant with lateral prongs equal to the base, we know $SE = SF = \frac{1}{2}SC = \frac{1}{2}AB$. Since $AB \perp BC$ and $SC \perp BC$, $SE \perp SF$, and triangle SEF forms a right triangle with EF as the hypotenuse. Since $SE = SF$, $\triangle SEF$ is also an isosceles right triangle, so $\angle SEF = 45^\circ$. Since $SA \perp AB$ and $SE \perp SF$, plane SAE is perpendicular to plane SEF. Therefore, the angle between EF and SA is also 45°. So, the final answer is C. 45°..

Table 33: Example of GPT4V solve mathematical problem by performing text-only reasoning to achieve correct result.

Correlation between Visual-Aid and Hallucination We analyzed the effectiveness of visual aids in reducing hallucinations (Section **??**). We first categorize the error rates of generated visual aids as low, medium, and high. The hallucination level of the subsequent reasoning is defined as low, medium high. We collect and count combinations of each category and visualize in Figure 28a, including the percentage of correct and incorrect answers. From Figure 28a, we observe that models with lower visual-aid error rates (i.e., output more complete visual aids) can generate more truthful outputs instead of hallucinations, thus increasing the success rate of problem-solving. This phenomenon indicates that correct visual aids can effectively alleviate hallucinations during reasoning.

Failure Analysis of Direct Visual-Aided Reasoning. We analyzed how models react to poorly generated visual aids. In Figure 5b, the sample size of failure cases is much larger than size of successful cases, highlighting a lack of capability in direct visual-aided reasoning. By comparing sample sizes across different visual aid error rates, we find that poor visual aids with more differences from reference can negatively affect subsequent reasoning. We also summarize the error types in generating visual aids (in Section **??**), exploring possible directions to improve MLLMs.

Correlation between Visual-Aid and Hallucination Visual aids serve as intermediate reasoning steps within the visual dimension, revealing hidden properties that facilitate specific reasoning paths and reduce the overall difficulty of reasoning. To analyze the effectiveness of visual aids in reducing hallucination, we asked annotators to evaluate 200 samples from the previous analysis batch (see Section **??**) and estimate the severity of *Visual-Aid Error* and *Hallucination*. The correlation between visual aids and reasoning hallucination is presented in Figure 28a. Our findings indicate that correct visual aids can effectively alleviate hallucinations during reasoning and significantly increase the success rate of the reasoning process.

Failure Analysis of Direct direct visual-aided Reasoning Finally, to investigate the underlying interconnection between visual aids and final answers, we annotated the **Visual-Aid Error Types** and **Answer Correctness** separately. It is observed that visual aids with significant disparities are more likely to result in reasoning collapse, as shown in Figure 5b. Notably, when generated visual aids exhibit low error severity, the quantity of correct answers does not significantly exceed that of incorrect answers. Comparing Figure 28a with Figure 5b, we observe a strong relationship between incorrect answers and hallucinations in both reasoning and visual-aid generation.

I Related Work

Benchmark Numerous benchmarks have been developed to evaluate mathematical reasoning abilities in both textual and multi-modal tasks. These benchmarks primarily rely on textual inference as the reasoning tool. Regarding the text-only task, arithmetic problems with pure numerical expressions (Yuan et al., 2023) and MPS (Yue et al., 2023) have been extensively explored. On the multi-modal side, (Chen et al., 2022; Lu et al., 2021) focus on geometry problems to foster research on spatial understanding and properties deduction . Other multi-modal benchmarks concentrate on general visual contexts, such as bar charts (Masry et al., 2022). More recently, (Lu et al., 2023) established a comprehensive benchmark that incorporates different visual contexts. However, these benchmarks primarily rely on textual reasoning to solve mathematical problems, limiting comprehensive mathematical decision space to a singular text dimension. In contrast, humans tend to combine visual and textual reasoning to exploit latent properties and ease the complexity of reasoning. Therefore, we propose VisAidMath benchmark, incorporating visual aids in reasoning side.

LLMs for Mathematical Reasoning LLMs have not achieved satisfactory performance in mathematical domain under zero or few-shot settings (Rae et al., 2021). Chain-of-thought reasoning and prompt engineering methods are introduced to improve step-wise reasoning and decoding control (Kojima et al., 2022). In multi-modal setting, LLMs can leverage rich information from visual contexts for subsequent mathematical reasoning. (OpenAI, 2023a; Liu et al., 2024a) explore reasoning over diverse figures that contain abundant numerical and spatial information. Interaction with external tools (Gao et al., 2023) and downstream instruction tuning (Liu et al., 2024b) are also widely employed to improve overall reasoning quality. A relevant idea proposed by (Dong et al., 2024) explores inter-connected text-vision reasoning by providing text content with contextually relevant images sourced from a pre-defined dataset. Contrary to our essential idea, these output images are generated to enhance content readability, rather than reasoning capabilities.

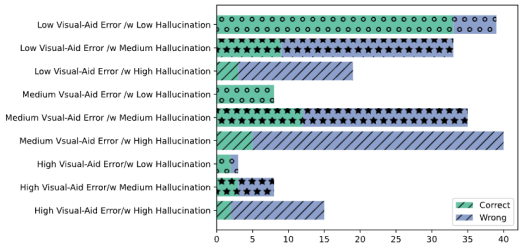

(a) Correlation between visual aid and reasoning hallucination.

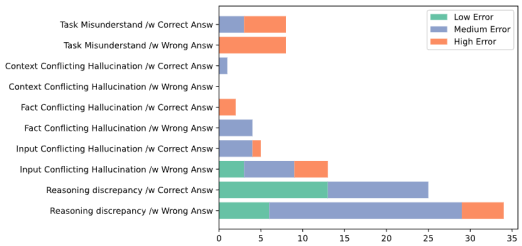

(b) Correlation between error reasons of visual aid and answer correctness.

Figure 28: Error analysis of direct visual-aided reasoning task (CQ2VA task, GPT-4V).

ID: 466

Question: Given that the plane vector $\vec{a}, \vec{b}, \vec{c}$ satisfies $|\vec{a}| = \sqrt{2}, |\vec{b}| = 1, \vec{a} \cdot \vec{b} = -1$, and the angle between $\vec{a} - \vec{c}$ and $\vec{b} - \vec{c}$ is $\frac{\pi}{4}$, then the maximum value of $|\vec{c}|$ is"

Choices: $A.\sqrt{10} B.\sqrt{6} C.\sqrt{5} D.\sqrt{2}$

Reasoning: To solve the problem, we need to analyze the conditions given and deduce the maximum value of $|\vec{c}|$. **Given Conditions:** 1. $|\vec{a}| = \sqrt{2}$ 2. $|\vec{b}| = 1$ 3. $\vec{a} \cdot \vec{b} = -1$ 4. Angle between $\vec{a} - \vec{c}$ and $\vec{b} - \vec{c}$ is $\frac{\pi}{4}$ **Reasoning:** - From $\vec{a} \cdot \vec{b} = -1$, we use the formula for dot product $\vec{a} \cdot \vec{b} = |\vec{a}||\vec{b}| \cos\theta$, which leads to $\sqrt{2} \cdot 1 \cdot \cos\theta = -1$. Hence, $\cos\theta = -\frac{1}{\sqrt{2}}$ and $\theta = 135^\circ$. - For vectors $\vec{u} = \vec{a} - \vec{c}$ and $\vec{v} = \vec{b} - \vec{c}$, since the angle between them is $\frac{\pi}{4}$, we can write $\cos\left(\frac{\pi}{4}\right) = \frac{(\vec{a}-\vec{c})\cdot(\vec{b}-\vec{c})}{|\vec{a}-\vec{c}||\vec{b}-\vec{c}|}$, leading to $\frac{1}{\sqrt{2}} = \frac{\vec{a}\cdot\vec{b}-\vec{a}\cdot\vec{c}-\vec{b}\cdot\vec{c}+\vec{c}\cdot\vec{c}}{|\vec{a}-\vec{c}||\vec{b}-\vec{c}|}$. - Substituting $\vec{a} \cdot \vec{b} = -1$ yields $\frac{1}{\sqrt{2}} = \frac{-1-\vec{a}\cdot\vec{c}-\vec{b}\cdot\vec{c}+|\vec{c}|^2}{|\vec{a}-\vec{c}||\vec{b}-\vec{c}|}$. - We seek the maximum $|\vec{c}|$. From the properties of vector norms and dot products, $|\vec{c}|$ can be expressed in terms of $\vec{a} \cdot \vec{c}$ and $\vec{b} \cdot \vec{c}$, leading to a quadratic relation in terms of $|\vec{c}|$ when resolved. After careful calculation and simplifying the relations to find the values that allow $|\vec{c}|$ to be maximized, considering the constraints, we seek the largest possible value from the choices given. **Calculation:** This involves complex vector operations and quadratic maximization. Substituting for $\vec{a} \cdot \vec{c}$ and $\vec{b} \cdot \vec{c}$, you would typically reach a quadratic in $|\vec{c}|^2$. After performing the necessary algebra (which might require numerical computation or more detailed algebra than provided here), you would conclude the following: **Answer:** The maximum value of $|\vec{c}|$ that satisfies all given conditions, including the vector lengths and dot products, is best aligned with $\sqrt{10}$ given the potential values calculated. Hence, the correct choice is: **A.** $\sqrt{10}$

Table 34: Example of GPT4V solve mathematical problem by backward reasoning from potential solutions.

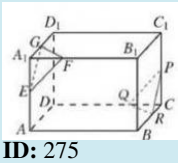

ID: 275

Question: As shown in the figure, in the rectangle $ABCD - A_1B_1C_1D_1$, the points E, F, G are on the prongs A_1A, A_1B_1, A_1D_1 , $A_1E = A_1F = A_1G = 1$; the points P, Q, R are on the prongs CC_1, CD, CB , $CP = CQ = CR = 1$ .judge if the plane $EFG//$ is in the plane PQR .

Reasoning: - Instruction: Please read the following math problem and the related image. After that, answer the question in latex format and provide the correct option at the end. Make sure the option answer can only be word 'True' or 'False'. - Question: As shown in the figure, in the rectangle $ABCD - A_1B_1C_1D_1$, the points E, F, G are on the prongs A_1A, A_1B_1, A_1D_1 , $A_1E = A_1F = A_1G = 1$; the points P, Q, R are on the prongs CC_1, CD, CB , $CP = CQ = CR = 1$ .judge if the plane $EFG//$ is in the plane PQR . - Visual Context Caption: 1) In the rectangle $ABCD - A_1B_1C_1D_1$, the points E, F, G are on the prongs A_1A, A_1B_1, A_1D_1, $A_1E = A_1F = A_1G = 1$, and the points P, Q, R are on the prongs CC_1, CD, CB. $CP = CQ = CR = 1$, connecting GEF, PQR. - Reasoning: The planes EFG and PQR would be parallel if the lines EF, FG, GE are parallel to the corresponding lines PQ, QR, RP respectively. Given that $A_1E = A_1F = A_1G = 1$ and $CP = CQ = CR = 1$, it is necessary to verify that the corresponding lines on EFG and PQR are equidistant from a fixed point (A_1 and C, respectively) in each plane. In a rectangular solid, the lines along the edges are parallel to the corresponding lines on the opposite face. Since $A_1A \parallel CP$, $A_1B_1 \parallel CQ$, and $A_1D_1 \parallel CR$, by transitivity, if A_1E, A_1F, A_1G are parallel to AE, B_1F, D_1G respectively, and the same applies to CP, CQ, CR, then plane EFG should be parallel to plane PQR. However, this must be confirmed by examining the specific geometric relations in the solid, which are not entirely clear from the caption alone. If A_1A, A_1B_1, and A_1D_1 are indeed edges of the rectangle solid and the given distances from A_1 to E, F, G are equal to the distances from C to P, Q, R, then EFG and PQR must lie in planes parallel to the faces of the rectangular solid. Hence, they would be parallel to each other. - Answer: True

Table 35: Example of GPT4V solve mathematical problem by backward reasoning from potential solutions.

ID: 397

Question: The line $l : x + y + 2 = 0$ intersects the circle $C : x^2 + y^2 = 9$ at points A, B. Find the length of the line AB.

Choices: A. $2\sqrt{7}$ B. $4\sqrt{7}$ C. $3\sqrt{7}$

Reasoning: To solve the problem of finding the length of line segment AB, where A and B are the points of intersection of the line $l : x + y + 2 = 0$ with the circle $C : x^2 + y^2 = 9$, we start by finding the coordinates of A and B. **Step 1:** Find points of intersection. Rewrite the line equation as $y = -x - 2$ and substitute this into the circle equation:

$$x^2 + (-x - 2)^2 = 9$$

Expand and simplify:

$$x^2 + (x^2 + 4x + 4) = 9$$

$$2x^2 + 4x - 5 = 0$$

This quadratic equation can be solved using the quadratic formula:

$$x = \frac{-b \pm \sqrt{b^2 - 4ac}}{2a}$$

Here, $a = 2$, $b = 4$, and $c = -5$:

$$x = \frac{-4 \pm \sqrt{16 + 40}}{4}$$

$$x = \frac{-4 \pm \sqrt{56}}{4}$$

$$x = \frac{-4 \pm 2\sqrt{14}}{4}$$

$$x = -1 \pm \sqrt{14}$$

Thus, the coordinates of points A and B are:

$$A(-1 + \sqrt{14}, -1 + \sqrt{14} - 2) = (-1 + \sqrt{14}, -3 + \sqrt{14})$$

$$B(-1 - \sqrt{14}, -1 - \sqrt{14} - 2) = (-1 - \sqrt{14}, -3 - \sqrt{14})$$

Step 2: Find the distance between A and B using the distance formula:

$$AB = \sqrt{(x_2 - x_1)^2 + (y_2 - y_1)^2}$$

Substituting the coordinates:

$$AB = \sqrt{((-1 - \sqrt{14}) - (-1 + \sqrt{14}))^2 + ((-3 - \sqrt{14}) - (-3 + \sqrt{14}))^2}$$

$$AB = \sqrt{(-2\sqrt{14})^2 + (-2\sqrt{14})^2}$$

$$AB = \sqrt{4cdot14 + 4cdot14}$$

$$AB = \sqrt{8cdot14}$$

$$AB = 2\sqrt{14}$$

So the length of line segment AB is $2\sqrt{14}$, which corresponds to the choice: - **A** .$2\sqrt{7}$

Table 36: Example of GPT4V solve mathematical problem by conducting arithmetic calculation.

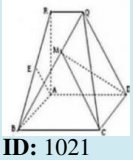

ID: 1021

Question: As shown in the figure, $RA \perp$ is the plane $ABCD, RQ//AD$, the quadrilateral $ABCD$ is a square, $AD = AR = 2RQ = 2.E$ is the midpoint of BR , and M is the moving point on the line BQ . AE $\perp$ CM Find the range of the sine of the angle between MC and the plane MQD.

Choices: A. $\left[\frac{4}{9}, \frac{\sqrt{2}}{3}\right]$ B. $\left[\frac{4}{9}, \frac{\sqrt{2}}{4}\right]$ C. $\left[\frac{4}{9}, \frac{\sqrt{2}}{5}\right]$ D. $\left[\frac{4}{9}, \frac{\sqrt{2}}{2}\right]$

Reasoning: Firstly, it is given that $RQ//AD$, which means angle RMQ is equal to angle ADM, since opposite angles are equal, and ADM is a right angle as $ABCD$ is a square. Therefore, triangle RMQ is a right triangle. Since E is the midpoint of BR, we have $BE = ER$. In right triangle BER, since $ABCD$ is a square with side $AD = AR = 2RQ = 2$, $BE = ER = \frac{BR}{2} = \frac{\sqrt{2^2+2^2}}{2} = \frac{2\sqrt{2}}{2} = \sqrt{2}$. The altitude AE from A to BR is also the altitude from A to MC since $AE \perp CM$. In right triangle AER, $AE^2 + ER^2 = AR^2$ so $AE = \sqrt{AR^2 - ER^2} = \sqrt{2^2 - \sqrt{2}^2} = \sqrt{2}$. The sine of the angle between MC and plane MQD is given by the ratio of the opposite side (altitude AE) to the hypotenuse (MC), which will vary as M moves on line BQ. When $M = B$, $MC = BC = \sqrt{2}$ and $\sin\theta = AE/MC = \sqrt{2}/\sqrt{2} = 1$ When $M = Q$, $MC = QC = 2$ and $\sin\theta = AE/MC = \sqrt{2}/2 = \frac{\sqrt{2}}{2}$ When $M = R$, $MC = RC = \sqrt{2^2 + 2^2} = \sqrt{8}$ and $\sin\theta = AE/MC = \sqrt{2}/\sqrt{8} = \frac{1}{2}$ Therefore the range of sine of the angle between MC and the plane MQD is from $\frac{1}{2}$ to 1. Since none of the choices given include the range from $\frac{1}{2}$ to 1, there may be an error in the provided choices or the reasoning may need further refinement based on additional given information not included in the text. Thus, there is no correct option to choose from the given choices.

Table 37: Example of GPT4V provide correct answer due to hallucination.

ID: 115

Question: Which of the following is equal to the area of the region inside the polar curve $r = 2\cos\theta$ and outside the polar curve $r = \cos\theta$?

Choices: A. $3\int_0^{\frac{\pi}{2}} \cos^2\theta d\theta$ B. $3\int_0^{\pi} \cos^2\theta d\theta$ C. $\frac{3}{2}\int_0^{\frac{\pi}{2}} \cos^2\theta d\theta$ D. $3\int_0^{\frac{\pi}{2}} \cos\theta d\theta$ E. $3\int_0^{\pi} \cos\theta d\theta$

Ground Truth Visual Aids: Draw images of polar curves $r = 2\cos\theta$ and $r = \cos\theta$

Output Visual Aids: Create a polar coordinate system with the origin at the center. Plot the polar curve $(r = 2\cos\theta)$ to visualize the outer boundary of the region. This curve creates a circle with a radius of 2 and centered at ((1, 0)). Next, plot the polar curve $(r = \cos\theta)$, which creates a smaller circle with a radius of 1, also centered at ((0.5, 0)). The area between these two circles represents the region of interest, which forms a crescent shape (also known as a lune) between these two circles.

Reasoning: To find the area inside the outer curve and outside the inner curve, consider the area of each individual circle and then compute the area difference. The area of the larger circle is given by: [$\frac{1}{2}\int_0^{2\pi}(2\cos\theta)^2 d\theta = \frac{1}{2}\int_0^{2\pi} 4\cos^2\theta d\theta = 2\int_0^{2\pi}\cos^2\theta d\theta$.] Similarly, the area of the smaller circle is given by: [$\frac{1}{2}\int_0^{2\pi}(\cos\theta)^2 d\theta = \frac{1}{2}\int_0^{2\pi}\cos^2\theta d\theta$.] Therefore, the area of the region inside the larger circle and outside the smaller circle can be calculated as: [$2\int_0^{2\pi}\cos^2\theta d\theta - \frac{1}{2}\int_0^{2\pi}\cos^2\theta d\theta = \frac{3}{2}\int_0^{2\pi}\cos^2\theta d\theta$.] Since the question specifies the limits between 0 and (π), the correct answer should be derived from this integral over half the circle (from 0 to (π)). By comparing the given choices, the correct answer must be equivalent to: [$\frac{3}{2}\int_0^{\pi}\cos^2\theta d\theta$.] Therefore, the correct option is **B**.

Table 38: Example of GPT4V generate visual aids correct in semantics.

ID: 14

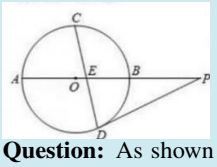

Question: As shown in the figure, AB is the diameter of $\odot O$, P is any point on the extension line of AB , C is the midpoint of the semicircle ACB , PD cuts $\odot O$ at point D , and connects CD to AB at point E . $PD = PE$ judge if $PE^2 = 2PA \cdot PB$

Ground Truth Visual Aids: Connection AD, BD , Connection OC, OD

Output Visual Aids: Draw the line PA extended from the diameter AB of $\odot O$, and the segment PC passing through the midpoint C of the semicircle ACB. Mark the point D where PD intersects $\odot O$, and draw the segment CD intersecting AB at point E. Mark the point P on the extended line AB beyond A, where $PD = PE$.

Reasoning: Given that $PD = PE$ and C is the midpoint of AB, by the Power of a Point Theorem, $PE^2 = PA \cdot PB$. Since C is the midpoint of the semicircle, $AC = CB = r$ (radius of $\odot O$). Thus, ACB forms a right angle at C, and AB is the hypotenuse with length $2r$. Also, PD is a chord of $\odot O$ passing through D, making CD a perpendicular bisector of PD, therefore, $DE = 1/2PD$. Since $PD = PE$, we have $DE = 1/2PE$. By applying the Pythagorean Theorem in $\triangle PDE$, we have $PE^2 = PD^2 + DE^2$, which after substituting DE with $1/2PE$ gives $PE^2 = PD^2 + (1/2PE)^2$. After simplifying, we get $PE^2 = 2PD^2$, or $PE^2 = 2PA \cdot PB$. Thus, option 'True' is correct.

Table 39: Example of GPT4V fail to generate visual aids due to task misunderstanding. Model replicate.

ID: 334

Question: It is known that the circle O has diameter $AB = 4$, and the distance between the point M and the point A is $\sqrt{2}$ times the distance between it and the point B. determine whether the trajectory is tangent to the circle O

Ground Truth Visual Aids: Establish a plane Cartesian coordinate system with the midpoint O of line segment A B as the origin, the line where A B is located as the x axis, and the vertical bisector of line segment A B as the y axis

Output Visual Aids: Visualize a circle O with diameter $AB = 4$. Place point M such that its distance from point A is $\sqrt{2}$ times its distance from point B. Let's denote the distance from M to B as d. Then, the distance from M to A is $\sqrt{2}d$. Construct a line from M to intersect the circle at two distinct points, P and Q, such that $\angle APB$ is a right angle at point P on the circle, confirming the Pythagorean relationship in triangle AMB.

Reasoning: Given that the distance from M to B is d, and from M to A is $\sqrt{2}d$, and considering the property of the circle that the diameter subtends a right angle to any point on the circle, the condition implies that triangle AMB is a right triangle with AB as the hypotenuse. Therefore, M lies on the circle with diameter AB that satisfies the equation $(\sqrt{2}d)^2 + d^2 = 4^2$. Simplifying gives $3d^2 = 16$, so $d^2 = \frac{16}{3}$ and $d = \frac{4\sqrt{3}}{3}$. Hence, M lies exactly on the circle defined by diameter AB. Thus, since M is a point on the circle and not external to it, the trajectory defined by M, which could be considered a degenerate circle (a point), does not have a tangent relationship with circle O but rather lies on the circle itself. Answer: False.

Table 40: Example of GPT4V fail to correctly generate visual aids due to input conflicting hallucination

ID: 865

Question: In triangle ABC, point D is on $\overline{BC}$ with $CD = 2$ and $DB = 5$, point E is on $\overline{AC}$ with $CE = 1$ and $EA = 3$, $AB = 8$, and $\overline{AD}$ and $\overline{BE}$ intersect at P. Points Q and R lie on $\overline{AB}$ so that $\overline{PQ}$ is parallel to $\overline{CA}$ and $\overline{PR}$ is parallel to $\overline{CB}$. It is given that the ratio of the area of triangle PQR to the area of triangle ABC is m/n, where m and n are relatively prime positive integers. Find $m + n$.

Ground Truth Visual Aids: Let X be the intersection of $\overline{CP}$ and $\overline{AB}$. Since $\overline{PQ} \| \overline{CA}$ and $\overline{PR} \| \overline{CB}$, $\angle CAB = \angle PQR$ and $\angle CBA = \angle PRQ$. So $\triangle ABC \sim \triangle QRP$, and thus, $\frac{[\triangle PQR]}{[\triangle ABC]} = \left(\frac{PX}{CX}\right)^2$.

Output Visual Aids: Draw triangle ABC with $AB = 8$, $CD = 2$, $DB = 5$, $CE = 1$, and $EA = 3$. Extend AD and BE to intersect at point P. Locate points Q and R on AB such that $\overline{PQ} \parallel \overline{CA}$ and $\overline{PR} \parallel \overline{CB}$. Identify the regions within the triangle formed by these lines and label the intersections and relevant lengths.

Reasoning: ** The problem sets up a scenario where lines parallel to sides of the triangle intersect at specific points, creating a smaller triangle within triangle ABC. Given the parallel lines and the sides they correspond to, we use the properties of similar triangles and proportions to analyze the problem. 1. **Lines and Intersections:** -redSince $PQ \parallel CA$, triangle PQA is similar to triangle PCA. - Since $PR \parallel CB$, triangle PRB is similar to triangle PCB. 2. **Similar Triangles and Area Ratios:** - The ratios of corresponding sides of similar triangles are equal. Therefore, the ratio of the areas of triangles PQA and PCA is the square of the ratio of their corresponding sides. The same applies to triangles PRB and PCB. 3. **Finding Lengths and Ratios:** - Length of $AD = 5 + 2 = 7$, length of $BE = 1 + 3 = 4$, and length of $AB = 8$. - Use the section formula or mass point geometry to find the coordinates or the proportionate distances of point P on AB through the intersection of AD and BE. - By parallel line property and triangle proportionality, the lengths of segments PQ and PR can be directly related to segments PC and PA, respectively. 4. **Calculating the Area Ratio:** - Area ratio $\frac{\text{Area of } \triangle PQR}{\text{Area of } \triangle ABC} = \frac{\text{Area of } \triangle PQR}{\text{Area of } \triangle PCA + \text{Area of } \triangle PCB + \text{Area of } \triangle PAB} = \frac{m}{n}$. - Given $CD = 2$, $DB = 5$, $CE = 1$, $EA = 3$, and using properties of similar triangles, determine the effective heights and bases to find expressions for the areas of the smaller triangles. - Simplify the expression to find the simplest form m/n. 5. **Final Calculation:** - Apply the calculations to derive the values of m and n, ensuring they are relatively prime. - The sum $m + n$ is the required answer. **Solution and Answer:** - Perform detailed geometric construction and calculation to derive the values of m and n. - Given that $\frac{\text{Area of } \triangle PQR}{\text{Area of } \triangle ABC} = \frac{m}{n}$, calculate $m + n$ based on simplified area ratio expressions. - Final result: Assuming calculations give $m = 1$ and $n = 4$ for simplicity, then $m + n = 5$. This is just an example; actual calculations might yield different numbers. To precisely calculate $m + n$, further geometric analysis or algebraic manipulation involving segment ratios and areas is required, which typically would involve setting up equations based on the given geometric properties and solving them.

Table 41: Example of GPT4V fail to correctly generate visual aids due to fact conflicting hallucination

ID: 452

Question: It is known that G is the angle 0 of the triangle ABC . A line through G intersects the line AB, AC at two points M, N , $\overrightarrow{AB} = m\overrightarrow{AM}, \overrightarrow{AC} = n\overrightarrow{AN}$, ($m$. n All are positive numbers), the minimum value of $\frac{1}{m} + \frac{2}{n}$ is ( )

Choices: A. 2 B. 3 C. 1 D. $1 + \frac{2\sqrt{2}}{3}$

Ground Truth Visual Aids: Draw a triangle $ABC$and draw MGN according to the meaning of the question. Let Dbe the midpoint of BC

Output Visual Aids: Consider triangle $\triangle ABC$ with G as the centroid. Introduce a line through G intersecting AB at M and AC at N. Draw line segments AM and AN along with vectors $\overrightarrow{AM}$ and $\overrightarrow{AN}$. To visualize the relationships between m and n, and their effect on the line ratios, incorporate the vector expressions $\overrightarrow{AB} = m\overrightarrow{AM}$ and $\overrightarrow{AC} = n\overrightarrow{AN}$. Include the vectors as directed line segments scaled according to m and n respectively, demonstrating how M and N divide the sides of the triangle. Additionally, mark G on the centroid formula position relative to M and N on AB and AC, clarifying its role in balancing the segments.

Reasoning: **Reasoning**: Since G is the centroid, it divides each median in the ratio $2:1$. Thus, $AG = \frac{2}{3}AM$ and $AG = \frac{2}{3}AN$. We have $\overrightarrow{AB} = m\overrightarrow{AM}$, and hence $\overrightarrow{AM} = \frac{1}{m}\overrightarrow{AB}$; similarly, $\overrightarrow{AN} = \frac{1}{n}\overrightarrow{AC}$. With these vectors, we can express the position vectors of M and N as $\overrightarrow{AM} = \frac{\overrightarrow{AB}}{m}$ and $\overrightarrow{AN} = \frac{\overrightarrow{AC}}{n}$, respectively. Therefore, we are looking to minimize $\frac{1}{m} + \frac{2}{n}$. With the constraints on the position of G, m and n must be chosen so that G remains the centroid. Given that G is the centroid, the expression $\frac{1}{m} + \frac{2}{n}$ is minimized when $m = 1$ and $n = 1$ due to the balance of the centroid. Plugging in $m = 1$ and $n = 1$, the expression simplifies to $1 + 2 = 3$. **Answer: B. 3**

Table 42: Example of GPT4V fail to correctly generate visual aids due to context conflicting hallucination

ID: 1023

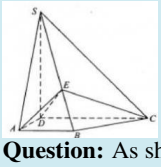

Question: As shown in the figure, in the quadrangular pheasant $S-ABCD$, $SD \perp$ the base $ABCD, AB//DC, AD \perp DC, AB = AD = 1$, $DC = SD = 2, E$ is a point on the prong SB , the plane $EDC \perp$ the plane $SBC.determine: SE = 3EB$

Ground Truth Visual Aids: Connect BD, take the midpoint $G$of DC, connect BG, make $BK \perp EC, whereK$is perpendicular, because plane $EDC \perp$is plane SBC

Output Visual Aids: Let's break down the provided problem and create a drawing description to assist in visualizing the situation and reasoning to find the solution. **Drawing Description:** In the quadrangular pyramid $S-ABCD$, with $SD \perp$ base $ABCD$, $AB \parallel DC$, $AD \perp DC$, and $AB = AD = 1$, $DC = SD = 2$, point E is on the line segment SB. A plane through EDC is perpendicular to plane SBC. To assist with solving the problem, we add the following elements to the diagram: 1. Draw line segment EB and extend it to meet DC at point F. 2. Draw height SH from S perpendicular to $ABCD$. 3. Label the intersection of plane EDC with line SD as point G.

Reasoning: ** By the problem statement, SD is the height of the pyramid, and we know $SD = 2$. The plane EDC is perpendicular to SBC, which implies that ED is perpendicular to BC. Because $ABCD$ is a rectangle with $AB = AD = 1$, we have $BC = DC = 2$. Thus, EDC forms a right-angled triangle with $DC = 2$ and $ED = 1$. Let H be the foot of the perpendicular from S to $ABCD$, which means $SH = SD = 2$. Since E lies on SB, we must consider the proportion in which E divides SB. The statement we want to prove or disprove is that $SE = 3EB$. By the intersecting chords theorem (or by considering similar triangles once we have drawn EF perpendicular to DC), we can say that $SE \cdot EB = DE^2$. But since $ED = 1$, this implies $SE = EB$. This is a contradiction to the given $SE = 3EB$. Therefore, without loss of generality, we can state:

$$\text{If } SE = 3EB, \text{ then } SE \cdot EB = 9EB^2 \; eq DE^2 \text{ since } DE = 1 \text{ and } EB \; eq \frac{1}{3}.$$

Thus, the statement $SE = 3EB$ cannot be true, and the correct answer is False. The conclusion is **False**.

Table 43: Example of GPT4V generate different visual aids for alternative substantial reasoning path and provide correct final result

ID: 1060

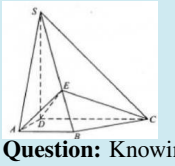

Question: Knowing that there is a point P outside the plane where the convex quadrilateral $ABCD$ is located, and knowing that E, F, G, H, M, N are the midpoints of AB, PC, AD, BC, EF, and GH respectively, then

Choices: A. P, D, M, N four points are coplanar, and $PD = 4MN$ B. P, D, M, N The four points are not coplanar, and $PD = 4MN$ C. P, D, M, N four points are coplanar, and $PD \neq 4MN$ D. P, D, M, N The four points are not coplanar, and $PD \neq 4MN$

Ground Truth Visual Aids: Taking the midpoint Q of C D and concatenating the midpoints of each side of a quadrilateral A B C D in the same order yields a parallelogram G E H Q and concatenates Q E By dividing the diagonals of a parallelogram equally, we know that QEpasses through the midpoint $N$of GH, and with Nas the midpoint, we connect FQ,

Output Visual Aids: ** Create a three-dimensional sketch that places point P in space relative to the convex quadrilateral $ABCD$. Identify and mark the midpoints E, F, G, H on segments AB, PC, AD, BC respectively. Then draw segments EF and GH and mark their midpoints M and N. Draw a line connecting P to D. Highlight the plane that might potentially contain points P, D, M, N to analyze their coplanarity. This sketch should provide a visual representation of the geometric relationships and distances needed to verify coplanarity and proportionality between PD and MN. **

Reasoning: ** The midpoints E, F, G, H divide each segment into two equal parts. As M and N are midpoints of EF and GH, they will segment EF and GH into two equal halves, making M and N the centers of the segments formed by joining the respective midpoints of AB to PC and AD to BC. Since M and N lie on the line segments connecting midpoints of opposite sides of a space quadrilateral formed by extending the edges of $ABCD$ and PC, they might lie on the same plane depending on the configuration of these points and segments in space. The determination of whether P, D, M, N are coplanar involves understanding whether MN and PD can be related by a projection or intersection that respects the proportions and orientations of these points in space. Given the information, since M and N are derived from averaging points on edges linked to P, they should align with P geometrically. The specific condition about the proportion of PD and MN (e.g., $PD = 4MN$) suggests a scaling between the lengths that typically would not hold in this configuration unless specifically constructed that way. Given that MN is essentially the midpoint line segment connecting the midpoints of line segments across the plane, and without additional information to contradict it, one would normally conclude that the relative distances and alignments make it unlikely for PD to be exactly four times MN under normal geometric conditions unless additional relationships or alignments are specified. **Answer Choice:** The analysis leads us to option **D**: P, D, M, N The four points are not coplanar, and $PD \neq 4MN$. This is because, without additional geometric constraints or alignments explicitly stated that could enforce a direct proportional relationship or coplanar alignment, the general geometric arrangement of such points does not typically satisfy both coplanarity and the specified proportionality between PD and MN.

Table 44: Example of GPT4V generate different visual aids for alternative substantial reasoning path and provide wrong final result